Reinvestigation of the elementary chemical kinetics of the reaction C2H5(•) + HBr (HI) → C2H6 + Br(•) (I(•)) in the range 293−623 K and its implication on the thermochemical parame...

ARTICLE *in* THE JOURNAL OF PHYSICAL CHEMISTRY A · NOVEMBER 2013

Impact Factor: 2.69 · DOI: 10.1021/jp403761r

3 AUTHORS, INCLUDING:

Michel J Rossi
Paul Scherrer Institut
259 PUBLICATIONS **6,612** CITATIONS

THE JOURNAL OF PHYSICAL CHEMISTRY A

Article

pubs.acs.org/JPCA

Reinvestigation of the Elementary Chemical Kinetics of the Reaction $C_2H_5^\bullet$ + HBr (HI) → C_2H_6 + $Br^\bullet$ ($I^\bullet$) in the Range 293−623 K and Its Implication on the Thermochemical Parameters of $C_2H_5^\bullet$ Free Radical

N. Leplat,[†] A. Wokaun,[‡] and M. J. Rossi*[,†]

[†]Laboratory of Atmospheric Chemistry (LAC) and [‡]General Energy Research (ENE) Division, Paul Scherrer Institute (PSI), CH-5232 Villigen PSI, Switzerland

ABSTRACT: A reinvestigation of the absolute rate constants of the metathesis reactions $C_2H_5^\bullet$ + HBr → C_2H_6 + $Br^\bullet$ (R1) and $C_2H_5^\bullet$ + HI → C_2H_6 + $I^\bullet$ (R2) has been performed and led to the following Arrhenius expressions: $k_1 = 3.69(\pm0.95) \times 10^{-11} \exp(-10.62(\pm0.66)/RT)$, $k_2 = 1.20(\pm0.38) \times 10^{-11} \exp(-7.12(\pm1.059)/RT)$ in the temperature range 293−623 K (A/cm^3 molecule^{-1} s^{-1}, E_a/kJ mol^{-1}). The study has been performed using a Knudsen reactor coupled to single-photon (VUV) photoionization mass spectrometer (SPIMS). Hydrocarbon free radicals have been generated externally before admission into the Knudsen reactor according to two different chemical schemes, enabling the generation of thermalized $C_2H_5^\bullet$ free radicals. A minor correction to k_1 and k_2 for the wall loss of $C_2H_5^\bullet$ (k_w) has been applied throughout the temperature range. The obtained results are consistent regarding both the disappearance of $C_2H_5^\bullet$ and the formation of closed shell products (n-C_4H_{10}, C_2H_4, C_2H_6), indicating that the chemical mechanism is largely understood and complete. Thermochemical parameters for $C_2H_5^\bullet$ free radical resulting from the present kinetic measurements are discussed and point toward a slightly lower value for the standard heat of formation $\Delta_f H^\circ_{298}(C_2H_5^\bullet)$ compared to some presently recommended values. On the basis of the present results and suitable data on the reverse reaction taken from the literature, we recommend $\Delta_f H^\circ_{298}(C_2H_5^\bullet)$ = 117.3 ± 3.1 kJ/mol resulting from an average of "third law" evaluations using $S^\circ_{298}(C_2H_5^\bullet)$ = 242.9 ± 4.6 J/K mol. The present work yields a standard heat of formation in satisfactory agreement with the results obtained by W. Tsang ($\Delta_f H^\circ_{298}(C_2H_5^\bullet)$ = 119 ± 2 kJ/mol) despite using two very different experimental techniques.

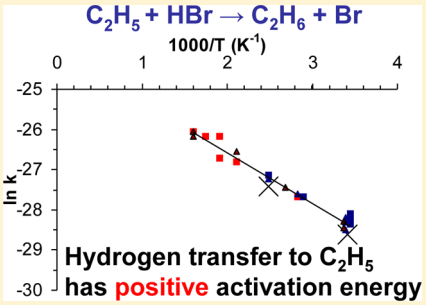

INTRODUCTION

Hydrocarbon free radicals are key chemical intermediates occurring in gas-phase or heterogeneous processes, such as combustion,[1] atmospheric chemistry, and microelectronic processing. Therefore, a better quantitative understanding of the chemistry in these processes requires an accurate knowledge of thermochemical quantities of the relevant free radicals including their standard enthalpy of formation $\Delta_f H^\circ_{298}(R^\bullet)$ and absolute entropy $S^\circ_{298}(R^\bullet)$. In the past, three experimental techniques were routinely used to determine these thermochemical quantities for a large set of free radicals, namely (i) the study of radical kinetics and equilibria, (ii) the use of gas-phase acidity cycles (positive ion cycles), and (iii) single-photon photoionization mass spectrometry (SPIMS) of radical anions (negative ion cycle).[2]

The landmark review article on hydrocarbon bond dissociation energies (BDE) by McMillen and Golden[3] contained the first collection of standard enthalpies of formation for many prototypical hydrocarbon free radicals $R^\bullet$ obtained by studying iodination equilibria such as $R^\bullet$ + HI ⇆ RH + $I^\bullet$ which remained unquestioned for a few years. The experimental base was laid by O'Neal and Benson, who obtained the first coherent set of values for many bond dissociation energies (BDEs) in the 1960s and 1970s.[4] Years before, Szwarc presented an extensive review of BDE values obtained using the toluene carrier technique which is now known to lead to erroneously low values of activation and thermochemical parameters.[5] The principal reason is thought to be that at the high temperature end toluene ceases to be a radical scavenger, thereby affording radical chain reactions in the flow system. However, a few years after publication of the McMillen and Golden[3] report, the accuracy of the BDE and $\Delta_f H^\circ_{298}(R^\bullet)$ were questioned by Pilling and co-workers, and others, in favor of higher values when new experimental techniques became available.[6] A few years later, Wing Tsang published an impressive series of thermochemical parameters for hydrocarbon free radicals whose thermochemical parameters were in fact significantly higher than the results displayed by McMillen and Golden.[7,8] Tsang made use of a single-pulse shock tube with subsequent stable product analysis that was used to deduce the chemical mechanism in the temperature range 1000−1200 K. The principal processes involved were hydrocarbon C−C bond scission and free radical combination/decomposition processes that overall confirmed the previously suspected high values for many free radicals. The most recent crop of results on the thermochemical parameters $\Delta_f H^\circ_{298}(R^\bullet)$

Received: April 16, 2013
Revised: October 14, 2013

   dx.doi.org/10.1021/jp403761r | J. Phys. Chem. A XXXX, XXX, XXX−XXX

Table 1. Obtained Rate Parameters for $C_2H_5^\bullet$ + HX (X = I, Br) → C_2H_6 + $X^\bullet$ and Corresponding $\Delta_f H°(R^\bullet)$ Based on the Corresponding $X^\bullet$ + C_2H_6 Rate Constants from the Literature

authors	A (cm^3 molecule^{-1} s^{-1})	E_a (kJ mol^{-1})	$\Delta_f H°_{298}(C_2H_5^\bullet)$ (kJ mol^{-1})
	$C_2H_5^\bullet$ + HBr → C_2H_6 + $Br^\bullet$		
Russell et al.[9]	1.00×10^{-12}	−3.4	120.0 ± 3.0
Nicovich et al.[12]	1.33×10^{-12}	−4.48	121.8 ± 2.1
Seakins et al.[10]	1.70×10^{-12}	−4.2	121.0 ± 1.5
Seetula[11]	1.87×10^{-12}	−3.7	120.7 ± 2.1
Dobis and Benson[14]	1.43×10^{-12}	1.85	118.7 ± 1.5
Ferrell[15]	1.94×10^{-12}	−3.42	121.5 ± 1.7
Fettis and Trotman-Dickenson[16]	$(1.06–8.3) \times 10^{-11}$ [a]	9.56	108.68
Golden et al.[17]	$k_{298\ K} = 7.0 \times 10^{-12}$		
	$C_2H_5^\bullet$ + HI → C_2H_6 + $I^\bullet$		
Hartley and Benson[18]	1.38×10^{-12}	4.60	105.75 ± 5.0
Seetula et al.[19]	4.5×10^{-12}	−3.19	117.0 ± 2.0

[a] Calculation based on the study of Fettis and Trotman-Dickenson,[16] in combination with more recent results of Hunter and Kristjansson,[20] and Hayes and Strong.[21]

were obtained using both bromination and iodination of $R^\bullet$ in a fast laminar flow tube coupled to SPIMS detection of the radical. This technique was pioneered by Gutman and implied free radical generation through photolysis of a suitable precursor using high-energy excimer laser radiation at 248 and 193 nm.[9−11] These experiments resulted in a consistent set of as yet highest values of $\Delta_f H°_{298}(R^\bullet)$ published to date. A variant of this technique of photolytic radical generation was used by Nicovich et al.,[12] who monitored atomic Br in the aftermath of the reaction $R^\bullet$ + HBr → RH + $Br^\bullet$ using resonance fluorescence of $Br^\bullet$. In several cases, agreement between results obtained from several determinations has not been achieved. As a consequence, the uncertainty of these values remains important, which hampers progress and is thus highly undesirable in view of the key role played by these important chemical intermediates.

Among these transient chemical species, ethyl radical $C_2H_5^\bullet$ is one of the intermediates commonly encountered in combustion and atmospheric chemistry. Its thermochemical parameters have previously been determined, notably using chemical equilibria. Here we will report on the experimental investigation of the kinetics of the following two elementary free radical−molecule metathesis reactions:

$$C_2H_5^\bullet + HBr \rightarrow C_2H_6 + Br^\bullet \quad (R1)$$

$$C_2H_5^\bullet + HI \rightarrow C_2H_6 + I^\bullet \quad (R2)$$

Together with their inverse rate constants that have been measured in the past, these investigations have provided equilibrium constants as a function of temperature enabling the extraction of the thermochemical parameters $\Delta_f H°_{298}(R^\bullet)$ and $S°_{298}(R^\bullet)$ for $C_2H_5^\bullet$. As may be seen from Table 1, the kinetics of the title reactions are still under debate today. The studies reporting small but positive activation energies have been more recently questioned in view of experimental results showing a negative temperature dependence associated with a significantly higher rate constant.[13] As a consequence of this disagreement, two sets of significantly different values of $\Delta_f H°_{298}$ and $S°_{298}$ for $C_2H_5^\bullet$ are found in the literature. From a fundamental point of view, the resolution of this problem is urgent in order to determine whether reactions of this type are elementary or complex or, in other words, occur either in a single step or two or more sequential steps.

The first direct measurement of the kinetics of the reaction between $C_2H_5^\bullet$ and HBr was performed by Russell et al.,[9] who reported a high rate of reaction associated with a negative activation energy (see Table 1). Experiments were performed in a tubular reactor coupled to a photoionization mass spectrometer. $C_2H_5^\bullet$ was produced by UV-flash photolysis of diethyl ketone using pulsed unfocused radiation at 193 nm from an excimer laser, and the free radical disappearance as a function of time upon reaction with HBr was measured in order to determine the reaction rate constant k_1. This initial investigation was later repeated by Seakins et al. using HBr at a higher level of purity.[10] This second study reported absolute values for the rate constant of reaction R1 that were approximately a factor of 2 higher than the original value obtained by Russell et al.[9] The Seakins et al. study[10] is in very good agreement with the results of Nicovich et al.[12] published a year before. The rate constant reported by Nicovich et al. was obtained by detecting $Br^\bullet$ atom appearance using resonance fluorescence spectroscopy. The $C_2H_5^\bullet$ was produced primarily by excimer laser flash photolysis of C_2H_5I at 266 nm, and by the slightly exothermic reaction C_2H_6 + $Cl^\bullet$ → $C_2H_5^\bullet$ + HCl for a single measurement performed at ambient temperature. This second source of $C_2H_5^\bullet$ radicals was used to show that the investigated reactions involved thermalized radicals. Indeed, as mentioned by Nicovich et al.,[12] important systematic errors in kinetic studies may arise because photolytic methods may generate radicals in excited (vibrational) states as pointed out notably in the review of Sato.[22] Recent experiments performed under similar conditions by Seetula,[11] where $C_2H_5^\bullet$ radicals were photogenerated at 248 nm from C_2H_5I inside a tubular flow reactor, support results obtained in these previous studies. In order to explain their results, the authors suggest a complex multistep mechanism involving a weakly bound complex just prior to a loose transition state. It has a lower potential energy compared to the reactants and, therefore, is consistent with the measured negative activation energy. The mechanism is discussed in more detail by Russell et al.[9] and Nicovich et al.[12] These kinetic studies supported a high value of $\Delta_f H°_{298}(C_2H_5^\bullet)$ lying between 120.7 and 121.8 kJ/mol. The value $\Delta_f H°_{298}(C_2H_5^\bullet)$ = 120 kJ/mol from Russell et al.[9] has been shown to be affected by a systematic error owing to the use of HBr of low purity.

In contrast, Dobis and Benson[14,23] reported experimental data that led to much lower rates and a positive activation

dx.doi.org/10.1021/jp403761r | J. Phys. Chem. A XXXX, XXX, XXX−XXX

energy for reaction R1, which in their opinion is the expected behavior for simple elementary metathesis reactions characterized by a single transition state. The thermochemical analysis of these results leads to a lower value of $\Delta_f H^\circ_{298}(C_2H_5^\bullet)$, namely 118.7 kJ/mol. The experiments were carried out in a very low pressure reactor (VLPR) using the $C_2H_6 + Cl^\bullet$ reaction as a thermal ethyl radical source. However, unlike Nicovich et al.,[12] $Cl^\bullet$ atoms were generated externally in a quartz discharge tube fitted with a microwave cavity upstream of the reactor and connected to it by a capillary inlet. Dobis and Benson claimed that the previously measured negative activation energies may arise from artifacts linked to the generation of "hot" free radicals excited by the laser flash system.[13−15,23]

One of the experimental studies on the kinetics of reaction R1 was an indirect measurement involving a set of reactions.[16] Diethyl ketone was photolyzed in a quartz reaction vessel in the presence of HBr and I_2, and the relative rates of reaction R1 and $C_2H_5^\bullet + I_2 \rightarrow C_2H_5I + I^\bullet$ were derived from the measurement of reactants and stable products involved in both reactions. By making the assumption that the reaction with I_2 has no activation energy, the authors found an activation energy of 9.56 kJ/mol for reaction with HBr. The thermochemical analysis performed by Fettis and Trotman-Dickenson leads to $\Delta_f H^\circ_{298}(C_2H_5^\bullet)$ = 108.7 kJ/mol. Unfortunately, the lack of kinetic data for the reaction of $C_2H_5^\bullet$ with I_2 has precluded an evaluation of the pre-exponential factor for reaction R1 as displayed in Table 1.

The first measurement of the rate constant k_2 of $C_2H_5^\bullet + HI \rightarrow C_2H_6 + I^\bullet$ was performed by Hartley and Benson.[18] They extracted the kinetic parameters for this reaction from experiments performed in a static reactor that involved the following set of reactions: $I_2 \leftrightarrows 2I^\bullet$, $C_2H_5I + I^\bullet \leftrightarrows C_2H_5^\bullet + I_2$, and $C_2H_5^\bullet + HI \leftrightarrows C_2H_6 + I^\bullet$. The Arrhenius plot determined from their experimental data shows a positive temperature dependence, with E_a = 4.6 kJ/mol for reaction R2, which leads to $\Delta_f H^\circ_{298}(C_2H_5^\bullet)$ = 105.8 kJ/mol in combination with the known rate constant for the reverse reaction. Their experimentally determined kinetic rate parameters are in fair agreement with preliminary evaluations from studies involving the same reaction system.[24,25]

More recently, the same experimental technique was used in refs 9 and 10; namely, a tubular reactor coupled to a photoionization mass spectrometer and photolytic generation of $C_2H_5^\bullet$ at 248 nm was used to perform a direct measurement of the kinetics of reaction R2.[19] Similar to their previous studies, checks have been performed in order to verify that relaxation of "hot" radicals occurred on a faster time scale compared to reaction and that the photolysis of HI by excimer laser radiation at 193 nm was kept to a minimum. The performed controls include the use of different free radical precursors, photolysis wavelengths, and bath gases (N_2 instead of He). In contrast to Hartley and Benson,[18] they obtained a negative activation energy for reaction R2 (E_a = −3.19 kJ/mol) and suggest $\Delta_f H^\circ_{298}(C_2H_5^\bullet)$ = 117.00 kJ/mol based on a "third law" treatment.

In addition to the above-mentioned experimental investigations, theoretical studies have been performed on the kinetics of reaction R1. A first ab initio study[26] found that this type of reactions, involving polar reactants such as HBr, proceeds via a weakly hydrogen-bonded intermediate complex $(R\cdots H\cdot X)^\bullet$ prior to formation of the transition state of lower energy. Their results and interpretation support the negative activation energies found experimentally. However, their predicted absolute rate constants are somewhat lower than the experimental results presented in refs 10−12, by approximatively 40 or 80% on the basis of transition state or RRKM theory. The theoretical study of Sheng et al.[27] also supports a complex mechanism for reaction R1, but with both a lower value of the rate constant and a much larger negative activation energy (−11.8 kJ/mol). Neither of those is consistent with the experimental findings. Furthermore, the energy difference between reactants and products leads to $\Delta_f H^\circ_{298}(C_2H_5^\bullet)$ = 109.6 and 113.3 kJ/mol corresponding to two different theoretical results for $\Delta_r H^\circ_{298}$ when currently accepted values for the standard enthalpies of formation of the other compounds from Burcat et al. are used.[28] These values are in fact in better agreement with the evaluation of Fettis and Trotman-Dickenson[9] and may therefore not be considered completely consistent with the work of Seakins et al.[10] and Seetula.[11]

Finally, quantum calculations on the potential energy surface pertaining to reaction R1 were recently performed by Golden et al.[17] and lead to results similar to Sheng et al.[27] concerning the temperature dependence of k_1. However, Golden et al. obtain a significantly larger absolute value for k_1 in comparison to the experimental results of Seakins et al.[10] and Seetula.[11] In this work the classical energy at the G2(MP2) level of theory of the ethyl−HBr adduct corresponded to a binding energy of 9.7 kJ/mol which was separated by a small barrier of less than 2 kJ/mol from the products $C_2H_6 + Br^\bullet$. This "inner" transition state was stiffer than the adduct intermediate and quite naturally led to negative activation energies when treated as a chemical activation problem starting from the HBr adduct using the Multiwell suite of programs of J. R. Barker (University of Michigan). The pressure-insensitive absolute rate constants were too high by a factor of 4 at 300 K and were brought into agreement with experiment by lowering the binding energy to 5.5 kJ/mol. The fitted experiments corresponded to high values of k_1 that are higher than the present values by a factor of 15. Had they wanted to fit the present results at 300 K these authors would have had to reduce the binding energy even further, perhaps at the expense of the stability of the HBr adduct. Starting at roughly 800 K, the temperature dependence of k_1 became positive owing to increasing rotational energy with temperature that led to a positive barrier for the inner transition state. These theoretical results may essentially indicate an important energetic change taking place by switching between a negative and a positive T-dependence regime. The argument seems to be at which temperature this switching point may lie.

A thorough review of the literature thus shows that the debate about the kinetic parameters of k_1 and k_2 remains open at this point. The source of discrepancies between experimental studies reporting high rates of reaction associated with a negative activation energy and those with much lower rates and positive activation energies have not been indentified with certainty, despite the help of modern quantum calculations. As a consequence of that, an uncertainty still remains regarding $\Delta_f H^\circ_{298}(C_2H_5^\bullet)$. Furthermore, $C_2H_5^\bullet$ free radical is not the only alkyl free radical for which the thermochemistry is under debate. Substantial disagreement in the rate parameters depending on the experimental technique used, for reactions of the type $R^\bullet + HX\ (X_2) \rightarrow RH\ (RX) + X^\bullet$, for X = I or Br, have been identified for many alkyl radicals. Moreover, a negative temperature dependence has also been identified for several (but not all) other formally elementary reactions of the

dx.doi.org/10.1021/jp403761r | J. Phys. Chem. A XXXX, XXX, XXX−XXX

type $R^{\bullet} + Cl_2 \rightarrow RCl + Cl^{\bullet}$ as presented in previously published studies of Timonen et al.[29,30]

Therefore, the present experimental study has been undertaken in order to provide new insight into the kinetics of reactions R1 and R2. Special care has been taken to generate thermalized free radicals, thus avoiding photolytic radical generation schemes. Indeed, the relaxation to a thermalized free radical distribution has been discussed as a source of possible systematic error in experiments involving the photolysis of a precursor and has been proposed to justify the observed disagreement.[13] The reinvestigation of the kinetics of reactions R1 and R2 has required the construction of a new experimental apparatus that has enabled major improvements in comparison to previous studies, including notably the external generation of $C_2H_5^{\bullet}$ radicals, upstream of their introduction into the reactor, and a thorough understanding of the chemical kinetics occurring in the Knudsen flow reactor, including the behavior of the free radical and its reaction products in the presence of HX. We therefore emphasize (i) the measurement of rate constants k_1 and k_2 as a function of temperature, and (ii) the discussion of the thermochemical consequences for $C_2H_5^{\bullet}$ free radical. The present work is the most comprehensive study of the titration of $C_2H_5^{\bullet}$ free radical with HX (X = I, Br) to date, dealing with both the detection of the free radical depletion and the accumulation of closed shell products resulting from radical recombination/disproportionation, and offers the possibility to set up a mass balance that is critical for the verification of the reaction mechanism.

We would like to point out that $\Delta_f H^{\circ}_{298}(C_2H_5^{\bullet})$ values obtained using other existing experimental methods have been listed in several reviews. We will briefly summarize the trend of $\Delta_f H^{\circ}_{298}(C_2H_5^{\bullet})$ over time and specifically focus on "third law" values. McMillen and Golden[3] recommend $\Delta_f H^{\circ}_{298}(C_2H_5^{\bullet}) = 108 \pm 4$ kJ mol^{-1} in their review; however, Pilling and coworkers[6] claimed $\Delta_f H^{\circ}_{298}(C_2H_5^{\bullet}) = 118.6 \pm 2$ kJ mol^{-1} as a higher value in agreement with the results obtained by Tsang,[7,8] who recommended $\Delta_f H^{\circ}_{298}(C_2H_5^{\bullet}) = 119 \pm 2$ kJ mol^{-1}. As shown in Table 1, the recent results from the study of kinetic halogenation equilibria generally gather at the higher limit proposed by Tsang but stay within the error limits of the recommended value. Table 2 displays the most recent results in chronological order obtained by a variety of techniques in addition to halogenation equilibria (Table 1) and shows the experimental spread of $\Delta_f H^{\circ}_{298}(C_2H_5^{\bullet})$ values which has become significantly smaller in recent years. In our opinion the significance of the present work lies in the fact that the determination of $\Delta_f H^{\circ}_{298}(C_2H_5^{\bullet})$ using two very different methods, namely single pulse shock tubes (Tsang[7,8]) and Knudsen flow reactors, leads to identical results for the thermochemical parameters of a free radical within the uncertainty limits under conditions of a thermal distribution of free radicals and using a "third law" approach.

The results presented in this paper are part of a larger experimental campaign that concentrates on the kinetics of similar halogenation reactions involving several alkyl radicals ($C_2H_5^{\bullet}$, i-$C_3H_7^{\bullet}$, n-$C_3H_7^{\bullet}$, $C_3H_5^{\bullet}$, i- or s-$C_4H_9^{\bullet}$, t-$C_4H_9^{\bullet}$, $C_7H_7^{\bullet}$, ...). This will be the subject of further communications in the near future.

EXPERIMENTAL TECHNIQUE

The new experimental apparatus is schematically represented in Figure 1. It consists of a Knudsen flow reactor coupled to a single-photon (VUV) photoionization mass spectrometer (SPIMS). Hydrocarbon free radicals were generated before their introduction into the Knudsen reactor in a couple of glass tubes in series, both 14 mm in diameter (o.d.) and 150 (discharge) and 200 mm (reaction) long, respectively. The free radical generation was achieved according to two different chemical schemes, both based on atom abstraction, either reactions R3 and R4 or reactions R5 and R6, and involves the following steps:

$$Cl_2 + h\nu\ (\mu\text{-wave}) \rightarrow 2Cl^{\bullet} \quad \text{(R3)}$$

$$Cl^{\bullet} + C_2H_6 \rightarrow C_2H_5^{\bullet} + HCl \quad (\Delta_r H^{\circ}_{298} = -20.1\ \text{kJ/mol}) \quad \text{(R4)}$$

$$H_2 + h\nu\ (\mu\text{-wave}) \rightarrow 2H^{\bullet} \quad \text{(R5)}$$

$$H^{\bullet} + C_2H_5I \rightarrow C_2H_5^{\bullet} + HI \quad (\Delta_r H^{\circ}_{298} = -74.9\ \text{kJ/mol}) \quad \text{(R6)}$$

Table 2. Recent Experimental Values for the Standard Heat of Formation $\Delta_f H^{\circ}_{298}$ of Ethyl Free Radical in Chronological Order

authors	$\Delta_f H^{\circ}_{298}(C_2H_5^{\bullet})$ (kJ mol^{-1})	method[a]
McMillen and Golden (1982)[3]	108 ± 4	review and evaluation
Castelhano and Griller (1984)[31]	120 ± 5	KE, radical buffer in solution
Pacey and Wimalasena (1984)[32]	119 ± 2	KE, pyrolysis of C_2H_6
Cao and Back (1984)[33]	117 ± 4	KE, $H_2 + C_2H_5^{\bullet}$ equilibrium
Brouard et al. (1986)[6]	118.7 ± 1.7	KE, $H^{\bullet} + C_2H_4$
Russell et al. (1988)[9]	120 ± 3	KE, bromination equilibrium
Parmar and Benson (1989)[34]	118.4 ± 1.7	KE, $Cl^{\bullet} + C_2D_6$ equilibrium
Ruscic et al. (1989)[35]	120.1 ± 2.4	PIC, radical photoinionization
Seetula et al. (1990)[19]	117 ± 2	KE, iodination equilibrium
Nicovich et al. (1991)[12]	121.8 ± 2.1	KE, bromination equilibrium
Seakins et al. (1992)[10]	122.0 ± 1.7	KE, bromination equilibrium
Hanning-Lee et al. (1993)[36]	120.2 ± 0.9	KE, $H^{\bullet} + C_2H_4$ equilibrium
Dobis and Benson (1995)[23]	118.8 ± 2.1	KE, bromination equilibrium
Tsang (1996)[7,8]	119 ± 2	SPST, hydrocarbon decomposition
Dobis and Benson (1997)[14]	118.8 ± 1.0	KE, bromination equilibrium
Seetula (1998)[11]	120.7 ± 2.1	KE, bromination equilibrium
Ferrell (1998)[15 b]	121.5 ± 1.7	KE, bromination equilibrium
Bödi et al. (2006)[37]	120.7 ± 1.0	PIC, photoionization
Leplat and Rossi (2013)[c]	117.3 ± 3.1	KE, halogenation equilibrium

[a]KE, kinetic equilibrium study; PIC, positive ion cycle based on the measurement of free radical ionization energy and positive fragment appearance potential measurements; SPST, single pulse shock tube investigation of suitable hydrocarbon precursors. [b]This work is the only of its kind in which k_1 and k_{-1} have been measured using the same experimental technique and thus represents an increased degree of coherence; [c]Present work.

dx.doi.org/10.1021/jp403761r | J. Phys. Chem. A XXXX, XXX, XXX−XXX

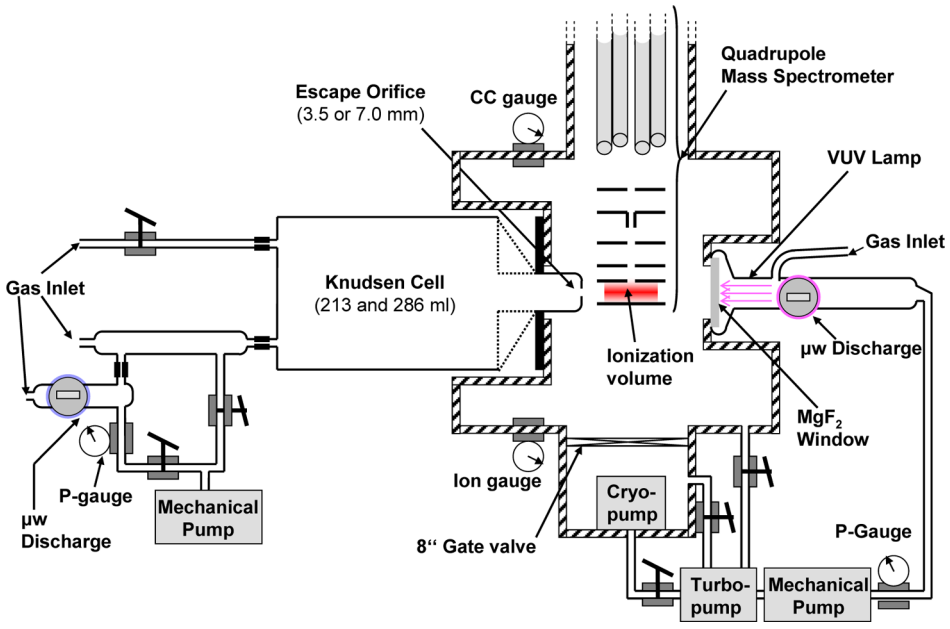

Figure 1. Schematic diagram of SPIMS instrument for free radical detection using VUV photoionization. Gas handling vacuum line (left) not shown.

Table 3. Important Parameters of the Knudsen Reactor

	reactor a	reactor b
volume (cm^3)	213	286
internal area (cm^2)	256	275.5
Φ (diam) of exit aperture (mm)	3.5	7.0
k_e (s^{-1})	$[1.034(\pm0.058)](T/M)^{1/2}$	$[2.367(\pm0.037)](T/M)^{1/2}$
ω (s^{-1})	$4386(T/M)^{1/2}$	$3509(T/M)^{1/2}$

$\Delta_r H^\circ_{298}$ for reactions R4 and R6 was calculated by using the thermochemical quantities listed in the database of Burcat et al.[28] including $\Delta_f H^\circ_{298}(C_2H_5^\bullet)$ = 119.6 kJ/mol. A flow of 20% H_2/Ar or 2−5% Cl_2/Ar mixture was established across the first tube at a working pressure in the range 0.1−0.3 mbar. This tube was excited by a 2.45 GHz microwave discharge in an Evenson microwave cavity. At 40 W power, approximately 50% and more than 80% of H_2 and Cl_2, respectively, underwent bond scission and generated $H^\bullet$ and $Cl^\bullet$ atoms in the discharge tube. This flow of atoms reacted downstream in a second (reaction) tube in the presence of a free radical precursor (C_2H_6 and C_2H_5I) in order to generate the hydrocarbon free radical of interest according to reaction R4 or R6. Subsequently, the free radicals and secondary products (HCl or HI) flowed into the Knudsen reactor and reacted with HX admitted across a separate inlet in an accurately measured flow whose purity was checked by MS. Back-diffusion from the reactor to upstream reaction vessels was prevented by the use of 1 mm i.d. inlet capillaries made of PTFE Teflon which are smaller in diameter than the exit apertures of the Knudsen cell toward the MS chamber. The glass (reaction) tube exposed to $C_2H_5^\bullet$ free radicals and the Knudsen reactor were coated by either Halocarbon Wax (15-00) or Teflon (FEP) in order to prevent or minimize free radical wall losses on the internal surface.

The external generation of $C_2H_5^\bullet$ is a key feature in our experimental approach and enables the generation of thermalized free radical for essentially two reasons: (i) there is no interaction of the direct precursors of $C_2H_5^\bullet$ (C_2H_6 or C_2H_5I) with the diffuse microwave plasma, and (ii) numerous "hard" collisions of $C_2H_5^\bullet$ with the vessel walls of the free radical generation tube will efficiently remove the excess internal energy of $R^\bullet$. It is therefore expected that all radicals flowing out of this vessel into the Knudsen reactor will be thermalized. Artifacts that may potentially lead to negative activation energies (E_a) and the associated abnormally large reaction rate constants when radicals are generated in situ by direct photolytic processes in the reactor are thus minimized or absent in view of the chemical free radical generation scheme. In addition, the use of a Knudsen reactor in which molecules undergo many thousands of efficient collisions (Z) with the reactor walls ($Z = \omega/k_e$, see below) rapidly cool the free radicals through transfer of the internal excitation of the free radicals.[38]

The gases escape from the reactor in an effusive molecular beam through an orifice of 3.5 or 7 mm nominal diameter into the MS chamber and were identified and quantitatively analyzed using single-photon SPIMS. Experiments were carried out using two different Knudsen reactors with the characteristics presented in Table 3. Reactor a is composed of two cylindrical parts: the first, with a diameter of 5.6 cm, is the main part of the reactor; the second constitutes an extension toward the ionization volume of the mass spectrometer. For reactor b, this extension is partially replaced by a conical part. The design differences between reactors a and b are represented by means of dashed lines in Figure 1. Both designs enable close proximity of the beam-forming exit orifice of the Knudsen reactor to the ionization volume of the quadrupole mass spectrometer (Balzers QMG421, QMA400 analyzer) in a direct line-of-sight coaxial geometry. Experiments were performed at different temperatures in the range 293−623 K thanks to a

dx.doi.org/10.1021/jp403761r | J. Phys. Chem. A XXXX, XXX, XXX−XXX

controller powering an electrical heating wire wound around the reactor and controlled by a type K thermocouple. The accuracy of the temperature reading is ±2 K.

The calibration of the escape rate constants k_e was performed using two different methods: (i) measurement of the disappearance of several pure inert gases of different molecular weights (H_2, CH_4, Ar, C_7H_8, and SF_6) as a function of time upon a sudden halt of the inlet flow, or (ii) accurate measurement of the steady state absolute pressure in the reactor using a Baratron type 627B as a function of a constant and measured inlet flow rate of the above-listed gases. These two methods are consistent with each other and enable the evaluation of k_e (s^{-1}) as a function of the molecular mass M (g/mol) at a given temperature T (K) according to $k_e = C_{st}(T/M)^{1/2}$ (see Table 3). The investigation of the kinetics using two flow reactors of different geometries enables the quantification of free radical losses on the internal walls of the Knudsen reactor in terms of the wall-loss rate constant k_w of the ethyl free radical.

Table 3 also reports the gas−wall collision frequency ω (s^{-1}). These experimental parameters were calculated following an estimate of the internal surface (A_{int}) and the measurement of the volume of the reactors resulting in the relation $\omega = 3.65 \times 10^3(A_{int}/V)(T/M)^{1/2}$.[38] The collision number (Z) of the average molecule with the wall of the reactor may be calculated from the calculated gas−wall collision frequency (ω) and the measured escape rate constant (k_e) as $Z = \omega/k_e$. The collision number is approximately equal to 4250 and 1500 in reactors a and b, respectively. The Knudsen number λ/Φ, where λ is the mean free path of the average gas molecule, is 44.1 at the highest used total pressure corresponding to 4.05×10^{12} molecules cm^{-3} (Table 5, first entry, sum of columns 7 and 11). All investigations have been performed under molecular flow conditions using the Knudsen number as a criterion.

Before mass separation and ion detection, the effusing gases were photoionized by a VUV discharge lamp sealed by a 2 mm thick, 1 in. diameter MgF_2 window, located on the opposite side of the MS chamber relative to the effusive molecular beam (see Figure1). VUV photons were obtained from discharging pure H_2 for Lyman α radiation (10.20 eV) or typically 1−2% (vol) Cl_2/He mixtures (8.87, 8.92 eV). The VUV photoionization enables accurate control of the ionization energy in comparison to electron impact at such low ionization energies and should completely prevent the detection of a MS signal coming from the fragmentation of heavier molecules. However, MS signals corresponding to fragmentation were detected in some cases, even if the photon energy was chosen to be lower than the fragmentation threshold for the heavier species. As an example, signals at m/z 28 and 29 of C_2H_6 appear when using H_2 or Cl_2 VUV discharge lamps despite high appearance potentials for $C_2H_5^+$ and $C_2H_4^+$ fragments from C_2H_6 of 12.5 and 12.1 eV, respectively.[39] These artifacts arise from the interaction between the incident VUV photons and external stainless steel surfaces of the ionizer that release photoelectrons owing to the photoelectric effect. These photoelectrons may induce fragmentation of closed shell molecules owing to field gradients within the ionizer volume. For the evaluation of the experiments performed so far, we have subtracted the MS intensity of the fragments when required, after suitable calibration, for example, the contribution at m/z 29 owing to fragmentation of C_2H_6 and C_2H_5I. For example, the fragment contribution may reach up to 70 or 85% of the total signal at m/z 29 for the precursors C_2H_6 and C_2H_5I, respectively. A complete description of the experimental apparatus as well as its performance limits will be published elsewhere.[40]

The used gases and liquids were provided by Messer (Ar ≥ 99.998%, H_2 ≥ 99.995%, HBr ≥ 99.98%, and C_2H_6 ≥ 99.95%), Air Liquide (Cl_2 ≥ 99.8%), Carbagas (C_2H_4 ≥ 99.95%), Fluka (C_4H_{10} ≥ 99%), and Sigma Aldrich (C_2H_5I ≥ 99%). The HI was prepared according to the procedure described by Dillon and Young.[41] All condensable gases (HBr, HI, Cl_2, and C_2H_5I) were purified and degassed by using several freeze (77.36 K)−pump−thaw cycles. The HI was stored in a glass bulb which was painted black in order to minimize photolytic decomposition into I_2 and H_2.

TREATMENT OF DATA

The data treatment must consider all relevant chemical and physical processes that can occur in the Knudsen reactor. Under the applied experimental conditions, the following chemical reactions are expected to take place:

$$C_2H_5^\bullet + HBr \rightarrow C_2H_6 + Br^\bullet \quad (R1)$$

$$C_2H_5^\bullet + HI \rightarrow C_2H_6 + I^\bullet \quad (R2)$$

$$C_2H_5^\bullet \rightarrow \text{wall loss} \quad (R7)$$

$$C_2H_5^\bullet + C_2H_5^\bullet \rightarrow C_2H_4 + C_2H_6 \quad (R8)$$

$$C_2H_5^\bullet + C_2H_5^\bullet \rightarrow n\text{-}C_4H_{10} \quad (R9)$$

Reactions R1 and R2 are the two reactions of interest competing with reactions R7, R8, and R9, namely the depletion of the ethyl free radical ($C_2H_5^\bullet$) by first-order wall loss (k_w), bimolecular disproportionation (k_d), and recombination (k_r) reactions, respectively.

As discussed below, this mechanism leads to a self-consistent picture of all experimental results and is an indication that there are no additional important secondary reactions in the mechanism that may have been neglected. The rate of reaction $C_2H_5^\bullet + X^\bullet \rightarrow C_2H_4 + HX$ (with $X^\bullet = Br^\bullet$ or $I^\bullet$) is slow compared to the rate of $C_2H_5^\bullet$ escape under the present experimental conditions. The reason is that $[C_2H_5^\bullet]$ is high at low concentrations of titrant when $[X^\bullet]$ is correspondingly low, whereas $[X^\bullet]$ reaches its maximum value when the majority of $C_2H_5^\bullet$ has been consumed by reaction with HX, reaction R1 or R2. At half-titration, when both $C_2H_5^\bullet$ and $X^\bullet$ were present at comparable concentrations, this reaction competed to the extent of only a few percent for the consumption of $C_2H_5^\bullet$ radical by HX, reactions R1 and R2. The potential hydrocarbon + $X^\bullet$ and hydrocarbon + $C_2H_5^\bullet$ reactions (with hydrocarbon = C_2H_4, C_2H_6, and n-C_4H_{10}) have been also considered and found to be negligible in view of their low rates of reaction given the rate constants found in the literature.[42] This includes the addition reaction Br + C_2H_4, which is in the falloff region with $k/k_\infty \leq 10^{-4}$ owing to the estimated small well depth (assuming C−Br bond dissociation energy in C_2H_4Br) of 37 kJ mol^{-1}.[42] Finally, as mentioned below under Results and Discussion, the experimental results indicated that no $Cl^\bullet$ or $H^\bullet$ radicals from the discharge tubes reached the reactor, and therefore, no further complications from the potential presence of highly reactive species are expected.

Two data evaluation procedures have been used in order to determine the rate constant k_i of interest, with i corresponding to either 1 or 2.

dx.doi.org/10.1021/jp403761r | J. Phys. Chem. A XXXX, XXX, XXX−XXX

Rate Constants Obtained from the Detection of Ethyl Radical. The first method is based on monitoring the MS parent peak of $C_2H_5^\bullet$ (m/z = 29) and its disappearance (depletion) as a function of the concentration of the titrant HBr or HI. In the chemical system described above, the variation of the concentration of $C_2H_5^\bullet$ is time independent at steady state conditions. Therefore, the source or inlet specific flow (in mol s^{-1} cm^{-3}), $R^{in}_{C_2H_5}$, or rate of ethyl appearance per time and volume unit, and the sink flow or rate of disappearance by reactions R1, R2, and R7−R9 or escape of the radical from the reactor, $k_e^{C_2H_5}$, are balanced as follows:

$$\frac{d[C_2H_5]}{dt} = R^{in}_{C_2H_5} - k_i[C_2H_5][HX] - 2(k_r + k_d)[C_2H_5]^2 - (k_w^{C_2H_5} + k_e^{C_2H_5})[C_2H_5] \equiv 0 \quad (1)$$

The exit specific flow of C_4H_{10} ($R^{out}_{C_4H_{10}}$) may be expressed by eq 2:

$$R^{out}_{C_4H_{10}} = k_r[C_2H_5]^2 \quad (2)$$

After substitution into eq 1, we obtain

$$\frac{d[C_2H_5]}{dt} = R^{in}_{C_2H_5} - k_i[C_2H_5][HX] - 2\left(1 + \frac{k_d}{k_r}\right)R^{out}_{C_4H_{10}} - (k_w^{C_2H_5} + k_e^{C_2H_5})[C_2H_5] \equiv 0 \quad (3)$$

Equation 3 can be rewritten in order to express specifically the concentration of the free radical:

$$[C_2H_5] = \frac{R^{in}_{C_2H_5} - 2\left(1 + \frac{k_d}{k_r}\right)R^{out}_{C_4H_{10}}}{k_i[HX] + (k_w^{C_2H_5} + k_e^{C_2H_5})} \quad (4)$$

Equation 4 transforms into eq 5 at initial conditions when [HX] = 0:

$$[C_2H_5]^0 = \frac{R^{in}_{C_2H_5} - 2\left(1 + \frac{k_d}{k_r}\right)R^{out,0}_{C_4H_{10}}}{k_w^{C_2H_5} + k_e^{C_2H_5}} \quad (5)$$

Dividing eq 5 by eq 4 we obtain the following relation:

$$\frac{[C_2H_5]^0}{[C_2H_5]} = \left(\frac{R^{in}_{C_2H_5} - \left(1 + \frac{k_d}{k_r}\right)2R^{out,0}_{C_4H_{10}}}{R^{in}_{C_2H_5} - \left(1 + \frac{k_d}{k_r}\right)2R^{out}_{C_4H_{10}}}\right) \times \left(1 + \frac{k_i}{k_w^{C_2H_5} + k_e^{C_2H_5}}[HX]\right) \quad (6)$$

We emphasize that the inlet and outlet specific flows R^{in} and R^{out} are the amounts that appear or disappear per time and unit volume flowing in or out of the reactor and are expressed in molecules s^{-1} cm^{-3}. As the concentration of $C_2H_5^\bullet$ is proportional to the intensity of the detected signal, the left term can be written as a ratio between the initial MS signal intensity of $C_2H_5^\bullet$ and the intensity at any titrant HX concentration, [HX].

Moreover, at the prevailing experimental conditions, the first term in parentheses on the right-hand side of eq 6 remains close to unity. This is the case when either $R^{in}_{C_2H_5}$ exceeds $2R^{out,0}_{C_4H_{10}}$ or when $R^{out,0}_{C_4H_{10}}$ does not strongly differ from $R^{out,0}_{C_4H_{10}}$. There is experimental evidence for the validity of these two constraints, and we have performed experiments accordingly by choosing conditions that follow at least one of these two conditions.

(i) The first evidence simply is an expression of the mass balance between the $C_2H_5^\bullet$ inlet flow and the specific outlet flows of all the chemical compounds and links $R^{in}_{C_2H_5}$ and $2R^{out,0}_{C_4H_{10}}$ by the following relation: $2R^{out}_{C_4H_{10}} = R^{in}_{C_2H_5} - R^{out}_{C_2H_5} - R^{out}_{C_2H_4} - (R^{out}_{C_2H_6} - R^{out}_{C_2H_6})$. Therefore, in any case, $R^{in}_{C_2H_5}$ is greater than $2R^{out,0}_{C_4H_{10}}$, especially when the extent of the radical−radical interaction is not too important. In the present experiment, consumption of 47% of $C_2H_5^\bullet$ was the largest measured disappearance of the free radical by self-reaction (see below). In that case, the ratio $2R^{out,0}_{C_4H_{10}}/R^{in}_{C_2H_5}$ may be estimated as 0.36 considering a ratio of 1/7 between disproportionation and recombination rate constants (see below).

(ii) The second condition, $R^{out,0}_{C_4H_{10}} \approx R^{out}_{C_4H_{10}}$, is met at small concentrations of the titrant HX. Therefore, we used mainly the data obtained at small [HX] for the rate constant determination.

(iii) When neither of these two conditions was fulfilled, a nonlinear response of eq 6 is expected when $I^0_{C_2H_5}/I_{C_2H_5}$ is plotted as a function of [HX] at high [HX]. Such a deviation from linearity was rarely observed and the data pertaining to these cases were not taken into account for the rate constant calculation.

(iv) As shown below, a complete calibration of the inlet and outlet specific flows of the chemical species, notably $R^{in}_{C_2H_5}$, $R^{out,0}_{C_4H_{10}}$, and $R^{out}_{C_2H_4}$, was performed for a few (marked) data sets. For these cases, it was numerically checked that the assumption of unity of the first term on the right-hand side of eq 6 does not lead to a significant change of k_i.

(v) The difference between $R^{in}_{C_2H_5}$ and $2R^{out,0}_{C_4H_{10}}$ is more important in reactor b (large aperture) than in reactor a. Indeed, $R^{out,0}_{C_4H_{10}}$ is smaller in reactor b owing to smaller $[C_2H_5^\bullet]$ at (nearly) identical inlet conditions. This was experimentally confirmed as the recorded MS signal for C_4H_{10} has not been unambiguously observed in reactor b given the prevailing signal-to-noise ratio of the MS spectrometer. Therefore, the validity of the hypothesis that the first term on the right-hand side of eq 6 is equal to 1 would be stronger for reactor b compared to a. The good agreement between results obtained in the two reactors (see below) may be interpreted as another indication of the fact that this assumption is well founded for both reactors.

For all the mentioned reasons (i)−(v), eq 6 may in the end be simplified as follows:

$$\frac{I^0_{C_2H_5}}{I_{C_2H_5}} = 1 + \frac{k_i}{k_w^{C_2H_5} + k_e^{C_2H_5}}[HX] \quad (7)$$

By plotting the ratio of the SPIMS signals given on the left-hand side of eq 7 as a function of the accurately measured HX concentrations, a linear regression line is obtained in which the slope is equal to $k_i/(k_w + k_e)$. [HX] was obtained by dividing the measured inlet flow of HX (in molecules s^{-1}), known from the measurement of the pressure depletion of HX in a calibrated volume located upstream to the reactor, by the

dx.doi.org/10.1021/jp403761r | J. Phys. Chem. A XXXX, XXX, XXX−XXX

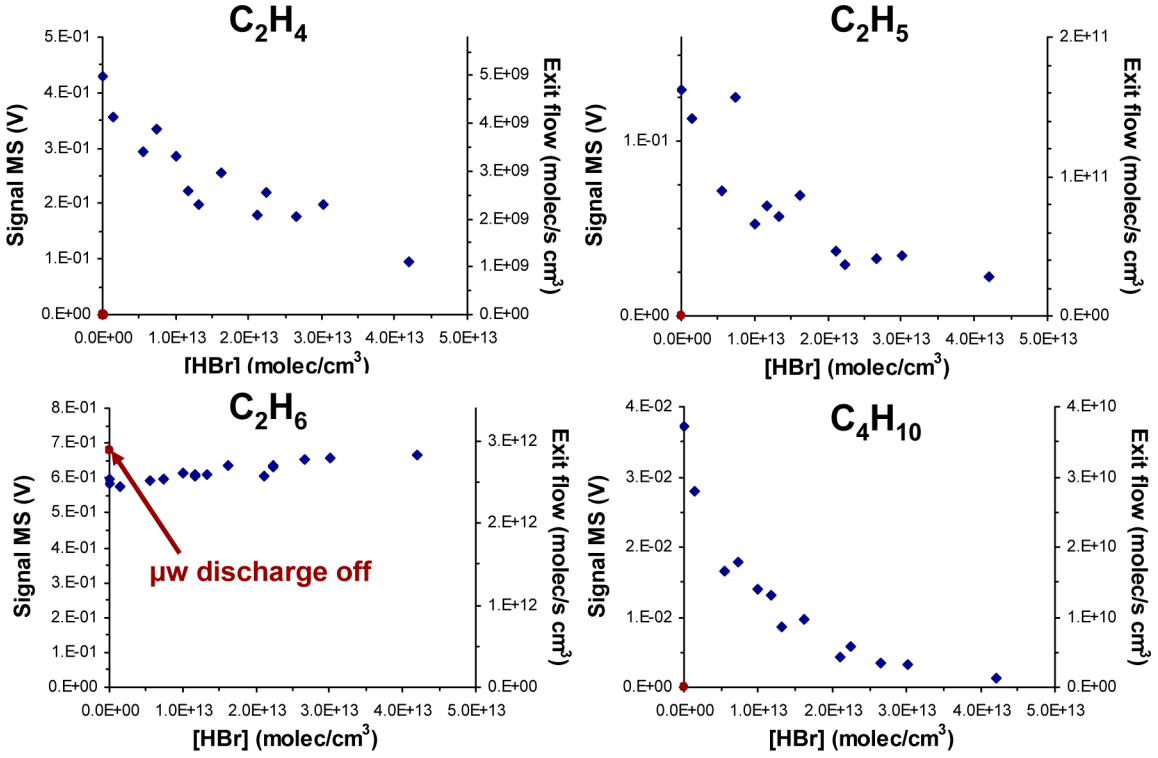

Figure 2. Functional dependence of C_2H_4, $C_2H_5^{\bullet}$, C_2H_6, and C_4H_{10} SPIMS signals and calibrated (C_2H_4, C_2H_6, and n-C_4H_{10}) and calculated ($C_2H_5^{\bullet}$) exit flows on the concentration of HBr in the Knudsen flow reactor (reactor a, 293 K, entry 5 in Table 5).

measured volume of the Knudsen reactor and k_e of HX. As k_e is known from calibration (Table 3) and by assuming that k_w is insignificant in comparison to k_e, the rate constant of interest (k_i) may easily be calculated from the regression line. The assumption $k_w < k_e$ is valid if experiments using two different Knudsen reactors with differing values of k_e lead to identical results for k_i within experimental uncertainty. For that reason, all experiments have been performed using two Knudsen reactors of different geometries using two escape orifices of different diameters. As presented below, a check on the absolute magnitude of k_w in relation to k_e has been performed at various temperatures. The experimental values for k_1 and k_2 have been corrected by taking into account the experimental values of k_w.

Rate Constants Obtained from Closed Shell Product Detection (CSPD). An alternative method for the derivation of the rate constant k_i is based on the detection of closed shell products of the chemical system given by reactions R1, R2, R7, R8, and R9, namely C_2H_4, C_2H_6, and C_4H_{10}. For these species, the escape flows are equal to the rates of production at steady state conditions, leading to

$$R^{\text{out}}_{C_4H_{10}} = k_r[C_2H_5]^2 \quad (2)$$

$$R^{\text{out}}_{C_2H_6} = R^{\text{in}}_{C_2H_6} + k_i[C_2H_5][HX] + k_d[C_2H_5]^2 \quad (8)$$

$$R^{\text{out}}_{C_2H_4} = k_d[C_2H_5]^2 \quad (9)$$

The following equation involving the closed shell products may be obtained from eqs 2, 8, and 9:

$$\frac{R^{\text{out}}_{C_2H_6} - R^{\text{in}}_{C_2H_6}}{R^{\text{out}}_{C_2H_4}} = 1 + \frac{k_i[HX]}{\frac{k_d}{\sqrt{k_r}}\sqrt{R^{\text{out}}_{C_4H_{10}}}} \quad (10)$$

The rate constant k_i in eq 10 is determined from the *change* of the left-hand ratio in eq 10 and $R^{\text{out}}_{C_4H_{10}}$ upon addition of HX. Using a suitable calibration for the SPIMS signals in terms of molecular flow of the closed shell species, and by taking currently accepted values from the literature for the rate of disproportionation and recombination reactions ($k_d = 2.01 \times 10^{-12}$ and $k_r = 1.42 \times 10^{-11}$ cm^3/molecules s) for $C_2H_5^{\bullet}$ free radical,[43] k_1 may be derived from a linear fit. This second method is more constrained as it requires the calibration of MS signals for several compounds. However, it has the advantage that k_{wall} does not need to be known. Furthermore, it is an ultimate and independent check that the chemical system of interest is completely understood. Indeed, if reactions would have been missed or failed to be taken into account in the relevant mechanism, the two methods of data evaluation would not be expected to agree.

Example of Data Processing. An example of the two different above-mentioned methods of data treatment may be illustrated using typical results obtained for the kinetics of reaction R1 at ambient temperature presented in Figure 2. In this example, which may be found in entry 5 of Table 5, $C_2H_5^{\bullet}$ free radicals were generated using $H^{\bullet}$ abstraction by atomic $Cl^{\bullet}$ according to reaction R4. The inlet flow rate of $C_2H_5^{\bullet}$ was 6.55×10^{13} molecules s^{-1} and was calculated by multiplying the measured inlet flow rate of C_2H_6 by the fraction of C_2H_6 that was consumed when the discharge was turned on. In reactor a of volume 213 cm^3 (Table 3), the specific inlet flow rate ($R^{\text{in}}_{C_2H_5}$) was equal to $6.55 \times 10^{13}/213 = 3.08 \times 10^{11}$ molecules/s cm^3. [HBr] was varied from 0 to 4.20×10^{13} molecules/cm^3. The partial pressure in the MS chamber was in the range 2.5×10^{-6}–3.5×10^{-6} Torr with a background value of 3×10^{-8} Torr. The experimental conditions in the Cl_2 discharge tube were 0.25 mbar partial pressure at 60 W leading to a Cl_2

dx.doi.org/10.1021/jp403761r | J. Phys. Chem. A XXXX, XXX, XXX–XXX

destruction of 75.2%. The photoionization lamp was operated on H_2 at 0.25 Torr and 70 W.

Figure 2 displays both the measured MS signal intensity and the specific exit flows (R_i^{out}) for the species considered. These values are obtained from suitable calibrations of C_2H_4, C_2H_6, and C_4H_{10} and calculated $C_2H_5^\bullet$ radical concentrations based on the MS signals of the involved above-mentioned closed shell species. Indeed, at the initial conditions, where [HBr] = 0, $[C_2H_5]$ may be calculated from eq 1 using the known escape rate constant $k_e^{C_2H_5}$, wall loss rate constant $k_w^{C_2H_5}$ (see below), inlet specific flow of the radical $R^{in}_{C_2H_5}$, and calibrated specific escape flows of C_2H_4 and C_4H_{10}. As $R^{out}_{C_4H_{10}} = k_r[C_2H_5]^2$ (eq 2) and $R_{C_4H_{10}}{}^{out} = k_d[C_2H_5]^2$ (eq 9), eq 1 may be rewritten as a flow balance in order to express $[C_2H_5]_{ss}$ as follows:

$$[C_2H_5]_{ss} = \frac{R^{in}_{C_2H_5} - 2R^{out}_{C_2H_4} - 2R^{out}_{C_4H_{10}}}{k_w^{C_2H_5} + k_e^{C_2H_5}} \quad (11)$$

This calculation leads to a steady state $C_2H_5^\bullet$ concentration $[C_2H_5]_{ss} = 4.97 \times 10^{10}$ molecules/cm^3 for [HBr] = 0, which corresponds to an outgoing specific flow of 1.64×10^{11} molecules/s cm^3 ($R^{out}_{C_2H_5} = R^{in}_{C_2H_5}[C_2H_5]_{ss}$). This calculated flow and the initial MS signal at m/z = 29 have been used as a calibration factor for $C_2H_5^\bullet$ which has allowed the calculation of the escape flow of this radical for any concentration of titrant, as presented in Figure 2. The comparison between the admitted and escaping $C_2H_5^\bullet$ specific flows, $R^{in}_{C_2H_5}$ and $R^{out}_{C_2H_5}$, indicates that, under the given conditions, 47% of the radical reacted by disproportionation, recombination, or wall loss in the absence of HBr.

The steady state concentration of $C_2H_5^\bullet$, $[C_2H_5]_{ss}$, may alternatively be obtained in a more direct way by solving eq 2 or 9, using the calibrated specific escape rate $R^{out}_{C_4H_{10}}$ or $R^{out}_{C_2H_4}$. This leads to steady state concentrations of $C_2H_5^\bullet$ equal to 5.14×10^{10} and 4.99×10^{10} molecules/cm^3, respectively, in the absence of HBr, which are in good agreement with the initial concentration of 4.97×10^{10} molecules/cm^3 derived above. It may also be noted that the specific outlet flow of C_2H_4 relative to C_4H_{10}, $R^{out}_{C_4H_{10}}/R^{out}_{C_2H_4} = 7.5$, is consistent with the ratio $k_r/k_d = 7.06$, as expected. These facts are good evidence that, in the absence of the titrant, the experimental results are completely consistent with the assumed mechanism and therefore strongly suggest that all major processes occurring in the reactor have been taken into account. Moreover, it indicates that wall loss does not generate substantial amounts of closed shell products. The wall loss is most probably a physical adsorption of ethyl radical, eventually followed by irreversible chemical reaction that does not release interfering gaseous products.

It may be seen in Figure 2 that approximately 10% of C_2H_6 is consumed upon turning on the Ar/Cl_2 μ-wave discharge with simultaneous production of $C_2H_5^\bullet$ in addition to C_2H_4 and C_4H_{10}. The latter two species are the products each of disproportionation (k_d) and recombination (k_r) reactions. Upon increase of the HBr concentration in the Knudsen reactor, $C_2H_5^\bullet$ is correspondingly consumed and turned into C_2H_6. As a consequence, both $C_2H_5^\bullet$ and the closed shell products C_2H_4 and C_4H_{10} decrease whereas the reaction product C_2H_6 increases and tends to the value measured with the discharge turned off, as expected.

By plotting the ratio of the $C_2H_5^\bullet$ SPIMS signals on the left side of eq 7 as a function of the concentration of HBr, a linear regression line with a slope equal to $k_1/(k_w^{C_2H_5} + k_e^{C_2H_5})$ is obtained. Figure 3 shows such a plot for the data displayed in Figure 2. The rate constant of reaction R1 is determined as $k_1 = [1.08(\pm0.34) \times 10^{-13}](k_w^{C_2H_5} + k_e^{C_2H_5}) = (1.08 \times 10^{-13})(\sim0 + 3.29) = 3.55(\pm1.11) \times 10^{-13}$ cm^3 molecules^{-1} s^{-1} for the reaction using the measured value of $k_e^{C_2H_5}$ and assuming that $k_w^{C_2H_5}$ is insignificant in comparison to $k_e^{C_2H_5}$. This latter assumption will be validated when similar experiments using a Knudsen reactor with a different value of $k_e^{C_2H_5}$ lead to results for k_1 identical within experimental uncertainty. It is shown below that a comparison of two independent data sets has enabled the measurement of the two unknowns, namely k_i and $k_w^{C_2H_5}$.

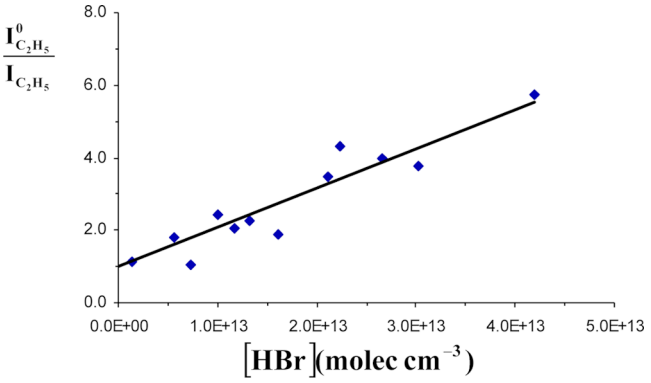

Figure 3. Linear regression line for I^0/I as a function of [HBr] used to derive the rate constant for $C_2H_5^\bullet + HBr \rightarrow C_2H_6 + Br^\bullet$. Correlation parameters (solid line): $y = [1.08(\pm0.34) \times 10^{-13}]x + 1.0$, $r^2 = 0.88$ (reactor a, 293 K, entry 5 in Table 5).

The data in Figure 2 may also be used to derive the rate expression by using the alternative data processing method based on the observation of the closed shell products from disproportionation and recombination (C_2H_6, C_2H_4, and C_4H_{10}) and their variation with increasing HBr concentration. The linear fit obtained according to eq 10 is shown in Figure 4, using accepted values from the literature for the rates of disproportionation and recombination reactions (k_d and k_r).[43] The second method affords a rate constant $k_1 = 3.80(\pm1.53) \times$

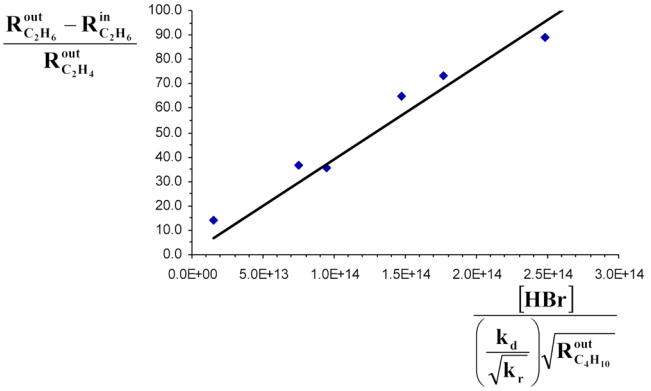

Figure 4. Linear fit for the measurement of the rate constant for $C_2H_5^\bullet + HBr \rightarrow C_2H_6 + Br^\bullet$ based on the observation of the concentration change of the closed shell products (CSPD) from disproportionation and recombination of $C_2H_5^\bullet$ free radical. Correlation parameters (solid line): $y = [3.80(\pm1.53) \times 10^{-13}]x + 1.0$, $r^2 = 0.959$ (reactor a, entry 5 of Table 5).

dx.doi.org/10.1021/jp403761r | J. Phys. Chem. A XXXX, XXX, XXX−XXX

Table 4. Kinetic Parameters for Reactors a and b, Evaluation of k_w, and Ratio k_w/k_e

reactor	A (cm^3/molecules s)	E_a (kJ/mol)	k_w (s^{-1}) 298 K	373 K	473 K	623 K	k_w/k_e min−max
		$C_2H_5^\bullet + HBr \rightarrow C_2H_6 + Br^\bullet$					
a	$(4.13 \pm 1.12) \times 10^{-11}$	11.57 ± 0.86	1.19	0.89	0.64	0.39	0.036−0.36
b	$(3.87 \pm 1.73) \times 10^{-11}$	11.01 ± 1.44					
		$C_2H_5^\bullet + HI \rightarrow C_2H_6 + I^\bullet$					
a	$(1.14 \pm 0.48) \times 10^{-11}$	7.43 ± 1.42	0.81	0.71	0.63	0.57	0.052−0.24
b	$(1.15 \pm 0.24) \times 10^{-11}$	7.17 ± 0.67					

10^{-13} cm^3 molecule^{-1} s^{-1}, which is a value in good agreement with the results of the first method based on the direct observation of $C_2H_5^\bullet$ free radical.

It has to be noted that the fits presented in Figures 3 and 4 have been constrained to go through unity intercept. It was verified that, over the whole set of experimental conditions, this constraint does not significantly change the slope (at most a few percent). Moreover, the corresponding slight changes do not lead to a systematic decrease or increase of the slope. Therefore, the obtained overall Arrhenius parameters are not significantly affected by this constraint.

Finally, these data, presented as typical results, may be used to illustrate that the reaction $C_2H_5^\bullet + Br^\bullet \rightarrow C_2H_4 + HBr$ (with $X^\bullet = Br^\bullet$ or $I^\bullet$) does not significantly affect the measurement of k_1. With a rate constant $k = 1.2 \times 10^{-11}$ molecules cm^{-3} s^{-1} according to Dobis and Benson,[14] this reaction may effectively compete for the pool of $C_2H_5^\bullet$ free radicals. At the 50% titration point, when both reactants are present in significant amounts, $[C_2H_5]_{ss} = [Br]_{ss} = 2.5 \times 10^{10}$ molecules/cm^3 may be estimated, which corresponds to half the initial $[C_2H_5]_{ss}$ calculated above. Figure 2 indicates that the half-titration point was at $[HBr]_{ss} \approx 1.5 \times 10^{13}$ molecules/cm^3. With $k_1 = 5.5 \times 10^{-13}$ at 298 K, corresponding to the average in the present study (see Table 5), the rate of removal of $C_2H_5^\bullet$ with Br and HBr would be $(2.5 \times 10^{10})(1.2 \times 10^{-11}) = 0.3$ s^{-1} and $(1.5 \times 10^{13})(5.5 \times 10^{-13}) = 8.25$ s^{-1}, respectively. The consumption of $C_2H_5^\bullet$ with $Br^\bullet$ is a small fraction of $k_e = 3.32$ s^{-1} and competes only to the extent of 3.5% with reaction R1 for the consumption of $C_2H_5^\bullet$. We therefore did not take into account the reaction of $X^\bullet + C_2H_5^\bullet \rightarrow C_2H_4 + HBr$ (with $X^\bullet = Br^\bullet$ or $I^\bullet$) because its contribution is deemed to be smaller than the experimental uncertainty of k_1.

Explicit Evaluation of k_w. Two independent data sets obtained in two Knudsen reactors of different geometries using the method based on the depletion of the ethyl free radical enables the evaluation of its wall loss over the whole temperature range. Indeed, the two reactors only differ in $k_e^{C_2H_5}$ ($k_e^{C_2H_5,a}$ and $k_e^{C_2H_5,b}$) that are accurately calibrated using stable gases owing to the use of two different nominal sizes of the escape orifice. For each reaction, two different linear Arrhenius plots have been obtained from measurements in each reactor, namely a and b. Table 4 displays Arrhenius parameters obtained from data presented in Tables 5 and 6. It may be noted that both pre-exponential terms and activation energies are in agreement within a statistical precision of 2σ over the whole range of investigated temperatures.

However, small but significant discrepancies remain between the two obtained Arrhenius plots suggesting a competitive, albeit small contribution of a radical loss process, presumably with the vessel walls. A numerical evaluation of k_w under the used experimental conditions was therefore performed. From the linear regression given in eq 7, the average value of the experimental slope S of $I^0_{C_2H_5}/I_{C_2H_5}$ as a function of [HX] at a given temperature is linked to $k_w^{C_2H_5}$, $k_e^{C_2H_5}$, and k_i according to the following equations:

$$S^a = \frac{k_i}{k_e^{C_2H_5,a} + k_w^{C_2H_5}} \quad (12)$$

$$S^b = \frac{k_i}{k_e^{C_2H_5,b} + k_w^{C_2H_5}} \quad (13)$$

Note that the superscripts "a" and "b" refer to the reactor. Equations 12 and 13 contain two unknowns, namely $k_w^{C_2H_5}$ and k_i, that may be determined from two significantly different pairs of S and $k_e^{C_2H_5}$ values, namely S^a and $k_e^{C_2H_5,a}$, and S^b and $k_e^{C_2H_5,b}$. In algebraic terms, one determines $k_w^{C_2H_5}$ that leads to an identical value of $k_i$in both reactors as expressed in eq 14:

$$k_i = S^a(k_e^{C_2H_5,a} + k_w^{C_2H_5}) = S^b(k_e^{C_2H_5,b} + k_w^{C_2H_5}) \quad (14)$$

from which $k_w^{C_2H_5}$ may be isolated and calculated as shown in eq 15:

$$k_w^{C_2H_5} = \frac{S^b k_e^{C_2H_5,b} - S^a k_e^{C_2H_5,a}}{S^a - S^b} \quad (15)$$

In the same way, it may be shown that a single value of $k_i$may be obtained at a given value of $k_w^{C_2H_5}$ at a given temperature following eq 16:

$$k_i = \frac{S^a S^b}{S^a - S^b}(k_e^{C_2H_5,b} - k_e^{C_2H_5,a}) \quad (16)$$

Therefore, by solving eqs 15 and 16, $k_w^{C_2H_5}$ as well as k_i may be calculated taking into account wall losses of $C_2H_5^\bullet$. The results of this calculation of $k_w^{C_2H_5}$are shown in Table 4 for several temperatures. It appears that the calculated wall losses k_w vary as a function of temperature from 0.40 to 1.19 s^{-1} and from 0.57 to 0.80 s^{-1}, for k_1 and k_2, respectively. The largest values of k_w are measured at ambient temperature, which corresponds to the lower limit of the investigated temperature range. The values of k_w represent at least 3.6% and at most 36% of the escape rate constant k_e. Therefore, the wall losses are not always insignificant, and experimental values have to be slightly corrected in order to take into account the presence of a small value of k_w. As a consistency check, the absolute magnitude of k_w is identical within experimental uncertainty in both Knudsen reactors (a and b) and is thus found to be independent of the presence of the titrant HX. It therefore appears that k_w describes the interaction of ethyl free radical with the vessel walls across the investigated temperature range.

RESULTS AND DISCUSSION

Present Experimental Results. The majority of the current measurements have been performed by monitoring

dx.doi.org/10.1021/jp403761r | J. Phys. Chem. A XXXX, XXX, XXX−XXX

Table 5. Experimental Conditions and Measured Rate Constants for $C_2H_5^\bullet$ + HBr → C_2H_6 + $Br^\bullet$

T (K)	wall coat.[a]	lamp[b]	$C_2H_5^\bullet$ prod	inlet flow of C_2H_5 (molecules s^{-1})	$[C_2H_5]_0$[c] (molecules cm^{-3})	$[HBr]_{max}$[d] (molecules cm^{-3})	k_1[e] (cm^3 s^{-1} $molecule^{-1}$)	k_1[f] (cm^3 s^{-1} $molecule^{-1}$)	error[g] (%)	n_0[h] (molecules cm^{-3})
Reactor a (V = 213 mL, Exit Aperture = 3.5 mm, k_{esc} (s^{-1}) = 1.034$(T/M)^{1/2}$)										
293	HCW	H_2	C_2H_6 + Cl	1.85×10^{14}	2.59×10^{11}	2.56×10^{13}	4.56×10^{-13}	6.21×10^{-13}	42	4.05×10^{12}
293	HCW	H_2	C_2H_6 + Cl	5.99×10^{13}	8.39×10^{10}	3.08×10^{13}	4.14×10^{-13}	5.64×10^{-13}	24	2.12×10^{12}
353	HCW	H_2	C_2H_6 + Cl	6.33×10^{13}	8.15×10^{10}	1.85×10^{13}	7.52×10^{-13}	9.53×10^{-13}	89	1.59×10^{12}
403	HCW	H_2	C_2H_6 + Cl	4.52×10^{13}	5.44×10^{10}	9.71×10^{12}	1.35×10^{-12}	1.63×10^{-12}	14	1.27×10^{12}
293	HCW	H_2	C_2H_6 + Cl	6.55×10^{13}	9.18×10^{10}	4.20×10^{13}	3.80×10^{-13} [i]	3.80×10^{-13} [i]	40	1.88×10^{12}
293	HCW	H_2	C_2H_6 + Cl	6.55×10^{13}	9.18×10^{10}	4.20×10^{13}	3.55×10^{-13}	4.84×10^{-13}	37	1.88×10^{12}
353	Tef	H_2	C_2H_6 + Cl	1.14×10^{14}	1.46×10^{11}	2.69×10^{13}	7.57×10^{-13}	9.58×10^{-13}	94	2.67×10^{12}
473	Tef	H_2	C_2H_6 + Cl	3.59×10^{13}	3.99×10^{10}	9.75×10^{12}	1.97×10^{-12}	2.26×10^{-12}	56	8.07×10^{11}
523	Tef	H_2	C_2H_6 + Cl	3.07×10^{13}	3.25×10^{10}	5.58×10^{12}	3.81×10^{-12}	4.28×10^{-12}	35	6.97×10^{11}
523	Tef	H_2	C_2H_6 + Cl	6.87×10^{13}	7.27×10^{10}	4.86×10^{12}	2.25×10^{-12}	2.52×10^{-12}	70	1.76×10^{12}
573	Tef	H_2	C_2H_6 + Cl	5.70×10^{13}	5.76×10^{10}	3.37×10^{12}	3.90×10^{-12}	4.29×10^{-12}	91	1.27×10^{12}
623	Tef	H_2	C_2H_6 + Cl	8.69×10^{13}	8.42×10^{10}	2.86×10^{12}	4.49×10^{-12}	4.86×10^{-12}	98	1.61×10^{12}
293	HCW	Cl_2	C_2H_5 I + H	3.47×10^{13}	3.08×10^{11}	3.03×10^{13}	4.16×10^{-13}	5.69×10^{-13}	37	3.02×10^{12}
293	HCW	Cl_2	C_2H_5 I + H	2.18×10^{14}	2.47×10^{11}	2.27×10^{13}	3.05×10^{-13}	4.18×10^{-13}	30	2.61×10^{12}
293	HCW	Cl_2	C_2H_5 I + H	1.76×10^{14}	5.91×10^{10}	2.02×10^{13}	3.67×10^{-13}	5.03×10^{-13}	65	5.68×10^{11}
353	HCW	Cl_2	C_2H_5 I + H	4.59×10^{13}	2.31×10^{10}	1.64×10^{13}	8.17×10^{-13}	1.03×10^{-12}	79	2.10×10^{11}
403	HCW	Cl_2	C_2H_5 I + H	1.92×10^{13}	2.97×10^{10}	9.87×10^{12}	1.24×10^{-12}	1.50×10^{-12}	25	3.16×10^{11}
403	HCW	Cl_2	C_2H_5 I + H	2.46×10^{13}	4.88×10^{10}	9.29×10^{12}	1.22×10^{-12} [i]	1.22×10^{-12} [i]	41	4.30×10^{11}
Reactor b (V = 287 mL, Exit Aperture = 7.0 mm, k_{esc} (s^{-1}) = 2.367$(T/M)^{1/2}$)										
293	Tef	H_2	C_2H_5 I + H	6.49×10^{13}	2.95×10^{10}	3.45×10^{13}	4.49×10^{-13}	5.22×10^{-13}	77	3.80×10^{11}
293	Tef	H_2	C_2H_5 I + H	4.01×10^{13}	1.82×10^{10}	2.63×10^{13}	3.79×10^{-13}	4.4×10^{-13}	44	2.44×10^{11}
373	Tef	H_2	C_2H_5 I + H	6.81×10^{13}	2.74×10^{10}	9.71×10^{12}	1.10×10^{-12}	1.21×10^{-12}	62	3.52×10^{11}
473	Tef	H_2	C_2H_5 I + H	7.21×10^{13}	2.58×10^{10}	8.18×10^{12}	2.74×10^{-12}	2.92×10^{-12}	70	3.29×10^{11}
623	Tef	H_2	C_2H_5 I + H	1.00×10^{14}	3.12×10^{10}	3.71×10^{12}	4.10×10^{-12}	4.24×10^{-12}	51	3.82×10^{11}
623	Tef	H_2	C_2H_5 I + H	5.61×10^{13}	1.75×10^{10}	3.64×10^{12}	4.67×10^{-12}	4.84×10^{-12}	53	2.28×10^{11}
Arrhenius Expressions for Whole Data Set										
$k_1 = 3.98(\pm0.86) \times 10^{-11} \exp(-11.35(\pm0.66)/RT)$ without k_w correction										
$k_1 = 3.69(\pm0.95) \times 10^{-11} \exp(-10.62(\pm0.66)/RT)$ with k_w correction										
A (cm^3/molecules s) and E_a (kJ/mol)										

[a]Wall coating material: Halocarbon Wax (HCW, 15-00) or Teflon (Tef, FEP). [b]Pure H_2 for Lyman α radiation (10.20 eV) or typically 1−2% Cl_2/He mixtures (8.87, 8.92 eV). [c]Obtained by dividing the inlet flow of C_2H_5 by Vk_e. The steady state concentration $[C_2H_5^\bullet]_{ss}$ is lower due to consumption of $C_2H_5^\bullet$ (up to 50%) by disproportionation and recombination. [d]The [HBr] range investigated is between zero (no HBr or "initial" conditions) and values tabulated. [e]Values of the rate constant obtained with the assumption $k_w = 0$. [f]Rate constant with k_w correction. [g]Error in the rate constants in percent of the absolute value of the rate constants. [h]n_0 is the initial total concentration based on the measured initial inlet flows of stable species and the known depletion ($\Delta[i]$) of these species (C_2H_6 or C_2H_5I and Cl_2 or HCl) when the μ-wave discharge is switched on and by considering the mass balance between the reactants and the product of the radical generation scheme ($\Delta[Cl_2]$ or $\Delta[H_2]$ = 1/2[HCl] or 1/2[HI] and $\Delta[C_2H_6]$ or $\Delta[C_2H_5I]$ = $[C_2H_5^\bullet]$. Therefore, $n_0 = [C_2H_5]_0 + [C_2H_6]_0$ or $[C_2H_5I]_0 + [HCl]_0$ or $[HI]_0 + [Cl_2]_0$ or $[H_2]_0 + [Ar]_0$. [i]Based on the detection of closed shell products (CSPD). See also graphs in Figures 2, 3, and 5.

the depletion of ethyl free radical ($C_2H_5^\bullet$). Other chemical species involved in the studied system such as C_2H_4, C_2H_6, C_4H_{10}, and Ar, as well as HBr, HI, HCl, and Cl_2 as the case may be, have also been monitored as a function of the measured

dx.doi.org/10.1021/jp403761r | J. Phys. Chem. A XXXX, XXX, XXX−XXX

Table 6. Experimental Conditions and Measured Rate Constants for $C_2H_5^\bullet$ + HI → C_2H_6 + $I^\bullet$

T (K)	wall coat.[a]	lamp[b]	$C_2H_5^\bullet$ prod	inlet flow of C_2H_5 (molecules s^{-1})	$[C_2H_5]_0$[c] (molecules cm^{-3})	$[HI]_{max}$[d] (molecules cm^{-3})	k_2[e] (cm^3 s^{-1} $molecule^{-1}$)	k_2[f] (cm^3 s^{-1} $molecule^{-1}$)	error[g] (%)	n_0[h] (molecules cm^{-3})
Reactor a (V = 213 mL, Exit Aperture = 3.5 mm, k_{esc} (s^{-1}) = $1.034(T/M)^{1/2}$)										
295	HCW	H_2	C_2H_6 + Cl	1.28×10^{14}	1.80×10^{11}	2.50×10^{13}	6.61×10^{-13}	8.20×10^{-13}	63	3.12×10^{12}
353	HCW	H_2	C_2H_6 + Cl	4.52×10^{13}	5.82×10^{10}	9.38×10^{12}	8.32×10^{-13}	1.00×10^{-12}	50	1.36×10^{12}
403	HCW	H_2	C_2H_6 + Cl	4.52×10^{13}	5.44×10^{10}	8.28×10^{12}	1.15×10^{-12}	1.35×10^{-12}	52	1.22×10^{12}
523	Tef	H_2	C_2H_6 + Cl	4.57×10^{13}	4.83×10^{10}	7.56×10^{12}	1.88×10^{-12}	2.14×10^{-12}	73	8.73×10^{11}
573	Tef	H_2	C_2H_6 + Cl	3.57×10^{13}	3.61×10^{10}	5.45×10^{12}	3.17×10^{-12}	3.58×10^{-12}	36	7.60×10^{11}
623	Tef	H_2	C_2H_6 + Cl	5.17×10^{13}	5.01×10^{10}	5.46×10^{12}	2.24×10^{-12}	2.50×10^{-12}	56	9.50×10^{11}
623	Tef	H_2	C_2H_6 + Cl	6.23×10^{13}	6.03×10^{10}	4.83×10^{12}	3.29×10^{-12}	3.68×10^{-12}	48	1.06×10^{12}
623	Tef	H_2	C_2H_6 + Cl	3.21×10^{13}	3.11×10^{10}	5.10×10^{12}	2.98×10^{-12}	3.34×10^{-12}	60	5.87×10^{11}
295	HCW	Cl_2	C_2H_5 I + H	5.80×10^{13}	8.17×10^{10}	3.22×10^{13}	5.11×10^{-13} [i]	5.11×10^{-13} [i]	50	7.80×10^{11}
295	HCW	Cl_2	C_2H_5 I + H	5.49×10^{13}	7.73×10^{10}	2.52×10^{13}	7.90×10^{-13}	9.82×10^{-13}	41	7.09×10^{11}
353	HCW	Cl_2	C_2H_5 I + H	3.81×10^{13}	4.90×10^{10}	9.62×10^{12}	7.23×10^{-13}	8.70×10^{-13}	63	4.63×10^{11}
403	HCW	Cl_2	C_2H_5 I + H	7.35×10^{13}	8.86×10^{10}	1.03×10^{13}	9.22×10^{-13}	1.08×10^{-12}	37	8.49×10^{11}
403	HCW	Cl_2	C_2H_5 I + H	3.20×10^{13}	3.85×10^{10}	9.75×10^{12}	1.04×10^{-12}	1.23×10^{-12}	17	3.51×10^{11}
403	HCW	Cl_2	C_2H_5 I + H	3.20×10^{13}	3.85×10^{10}	9.75×10^{12}	1.04×10^{-12} [i]	1.04×10^{-12} [i]	30	3.53×10^{11}
403	Tef	Cl_2	C_2H_5 I + H	4.93×10^{13}	5.94×10^{10}	7.12×10^{12}	1.45×10^{-12}	1.70×10^{-12}	44	6.03×10^{11}
623	Tef	Cl_2	C_2H_5 I + H	4.51×10^{13}	4.37×10^{10}	5.73×10^{12}	2.97×10^{-12}	3.31×10^{-12}	63	4.47×10^{11}
Reactor b (V = 287 mL, Exit Aperture = 7.0 mm, k_{esc} (s^{-1}) = $2.367(T/M)^{1/2}$)										
293	Tef	H_2	C_2H_5 I + H	6.73×10^{13}	2.01×10^{10}	2.27×10^{13}	5.74×10^{-13}	6.35×10^{-13}	80	3.71×10^{11}
293	Tef	H_2	C_2H_5 I + H	7.21×10^{13}	1.50×10^{10}	3.66×10^{13}	6.45×10^{-13}	7.13×10^{-13}	48	3.95×10^{11}
373	Tef	H_2	C_2H_5 I + H	3.52×10^{13}	1.42×10^{10}	8.65×10^{12}	1.11×10^{-12}	1.20×10^{-12}	91	1.80×10^{11}
473	Tef	H_2	C_2H_5 I + H	5.61×10^{13}	3.28×10^{10}	7.04×10^{12}	1.92×10^{-12}	2.05×10^{-12}	81	2.47×10^{11}
623	Tef	H_2	C_2H_5 I + H	4.81×10^{13}	3.06×10^{10}	3.01×10^{12}	2.76×10^{-12}	2.90×10^{-12}	41	1.86×10^{11}
623	Tef	H_2	C_2H_5 I + H	6.25×10^{13}	1.95×10^{10}	4.64×10^{12}	2.98×10^{-12}	3.13×10^{-12}	11	2.38×10^{11}
Arrhenius Expressions for the Whole Data Set										
$k_2 = 1.13(\pm0.33) \times 10^{-11} \exp(-7.319(\pm0.98)/RT)$ without k_w correction $k_2 = 1.20(\pm0.38) \times 10^{-11} \exp(-7.126(\pm1.059)/RT)$ with k_w correction A (cm^3/molecules s) and E_a (kJ/mol)										

[a]Wall coating material: Halocarbon Wax (HCW, 15-00) or Teflon (Tef, FEP). [b]Pure H_2 for Lyman α radiation (10.20 eV) or typically 1−2% Cl_2/He mixtures (8.87, 8.92 eV). [c]Obtained by dividing the inlet flow of C_2H_5 by Vk_e. The steady state concentration $[C_2H_5^\bullet]_{ss}$ is lower due to consumption of $C_2H_5^\bullet$ (up to 50%) by disproportionation and recombination. [d]The [HI] range investigated is between zero (no HI or "initial" conditions) and values tabulated. [e]Values of the rate constant obtained with the assumption k_w = 0. [f]Rate constant with k_w correction. [g]Error in the rate constants in percent of the absolute value of the rate constants. [h]n_0 is the initial total concentration based on the measured initial inlet flows of stable species and the known depletion ($\Delta[i]$) of these species (C_2H_6 or C_2H_5I and Cl_2 or HCl) when the μ-wave discharge is switched on and by considering the mass balance between the reactants and the product of the radical generation scheme ($\Delta[Cl_2]$ or $\Delta[H_2]$ = 1/2[HCl] or 1/2[HI] and $\Delta[C_2H_6]$ or $\Delta[C_2H_5I]$ = $[C_2H_5^\bullet]$. Therefore, $n_0 = [C_2H_5]_0 + [C_2H_6]_0$ or $[C_2H_5I]_0 + [HCl]_0$ or $[HI]_0 + [Cl_2]_0$ or $[H_2]_0 + [Ar]_0$. [i]Based on the detection of closed shell products (CSPD). See also graphs in Figures 2, 3, and 5.

flow rate of the titrant. The HCl and Cl_2 MS signals remained constant with the flow rate of HBr or HI when $C_2H_5^\bullet$ was generated using the reaction $Cl^\bullet + C_2H_6 \rightarrow C_2H_5^\bullet + HCl$. This suggests that no $Cl^\bullet$ radicals are admitted to the Knudsen reactor and that HX does not diffuse into the Cl_2 discharge tube or to the $Cl^\bullet + C_2H_6$ mixing region (radical mixing tube) where $C_2H_5^\bullet$ is produced. Therefore, the analysis does not seem to be subject to potential artifacts resulting from the reaction $HX + Cl^\bullet \rightarrow X^\bullet + HCl$, with X = Br or I, that occurs at a competitive rate owing to the large rate constant $k_{Cl+HI}(298\ K) = 1.22 \times$

dx.doi.org/10.1021/jp403761r | J. Phys. Chem. A XXXX, XXX, XXX−XXX

10^{-10} cm^3/molecule s measured by Yuan et al.,[44] or some other secondary reactions suggested by Dobis and Benson.[14] One of the important benefits of the external generation of $C_2H_5^\bullet$ performed using the new apparatus is the absence of complicating secondary reactions brought about by the presence of $Cl^\bullet$ or $H^\bullet$ atoms inside the Knudsen reactor. HBr and HI MS signals were monitored to confirm the linear dependence with the inlet flow, passing through the origin or slightly above in the case of HI when using the $H^\bullet + C_2H_5I \rightarrow C_2H_5^\bullet + HI$ generation scheme. Indeed, the HI flowing out the $C_2H_5^\bullet$ generation chamber in that case was negligible in comparison to the flow of HI used as titrant and may thus contribute to the small intercept when the flow of the HI titrant is set to zero. This is an additional check of the accuracy of the measurement of the inlet flow of HX. Ar signals used as an internal standard were monitored in order to check that each set of experiments was performed under controlled and stable conditions, especially regarding the photoionization yield.

Tables 5 and 6 list details of all experimental kinetic results obtained for reactions R1 and R2, respectively. The tabulated inlet flows of $C_2H_5^\bullet$ were calculated by multiplying the measured total inlet flows of the radical precursor (C_2H_6 or C_2H_5I) by the measured fractional decrease when the discharge was switched on and by an experimentally determined ratio that represented the branching ratio between the flow being pumped away and that admitted to the Knudsen reactor. Note that the tabulated inlet flows ($F^{in}_{C_2H_5}$ in molecules s^{-1}) enable the estimation of the (hypothetical) initial concentration of $C_2H_5^\bullet$ according to $[C_2H_5]_0 = F^{in}_{C_2H_5}/k_e^{C_2H_5}V$. Results obtained from such calculations are an upper limit for initial (=absence of HX) $[C_2H_5^\bullet]_{ss}$, because a fraction of $C_2H_5^\bullet$ will react by disproportionation (reaction R8) and recombination (reaction R9) at steady state conditions. Indeed, it was determined for experiments in which the exit flows of stable species were calibrated that $[C_2H_5^\bullet]_{ss}$ may be up to 40−50% smaller than $[C_2H_5^\bullet]_0$. The disproportionation and recombination reactions upstream of the reactor were kept low by maintaining a short residence time in the free radical generating tube owing to fast pumping. This feature was confirmed by the fact that only marginal signals for C_2H_4 and C_4H_{10} were detected for experiments performed in reactor b (7 mm). The initial inlet flow of $C_2H_5^\bullet$, $F^{in}_{C_2H_5}$, was measured both at the beginning and at the end of each set of individual rate constant measurements which were carried out by successively increasing and decreasing the flow of the titrant. No temporal variation of this key parameter was observed, which is evidence for good temporal stability of the operating conditions, notably regarding the μ-wave discharge properties. The total maximum concentration in the reactor is the sum of the concentrations in columns 7 and 11 in Tables 5 and 6, namely the sum of $[HX]_{max}$ and n_0, which has been used to confirm the molecular flow regime characterized by the Knudsen number (see above).

The fourth and third to last columns of Tables 5 and 6 list the expermimental rate constants with and without $k_w^{C_2H_5}$ corrections, respectively, described in the previous section. The results of the penultimate column are obtained using the assumption $k_w^{C_2H_5} = 0$. The present data suggest that $k_w^{C_2H_5}$ is small because of the following:

(i) The obtained rate constants are independent of the used wall coating (Halocarbon Wax or FEP Teflon). Therefore, the physicochemical properties of the reactor wall do not influence the results, as expected.

(ii) The results obtained using the closed shell product data treatment (CSPD), which does not depend on the wall loss for $C_2H_5^\bullet$ free radical, affords kinetic constants in excellent agreement with the evaluation following the direct observation of $C_2H_5^\bullet$ free radical when the assumption $k_w^{C_2H_5} = 0$ is made.

(iii) The kinetic parameters obtained in two different reactors are in agreement within the 2σ experimental uncertainties. These experimental observations strongly suggest that $k_w^{C_2H_5}$ is of minor importance for ethyl free radical in the present temperature range. However, we have decided to take $k_w^{C_2H_5}$ into account in the evaluation of k_1.

The explicit calculation of $k_w^{C_2H_5}$ has shown that it may attain a significant fraction of $k_e^{C_2H_5}$, especially at the lowest investigated temperatures. Therefore, we have applied a correction to k_1 and k_2 in order to take into account the slight effect of $k_w^{C_2H_5}$ on k_i. The corrected values of k_1 and k_2 are listed in the third from the last columns on the right side of Tables 5 and 6, respectively.

The Arrhenius plots of the present data are shown in Figures 5 and 6 along with a few typical uncertainty limits obtained from the standard deviation based on a least-squares analysis of the slopes of the experimental fits of the individual rate constants. The evaluation of uncertainties has been performed for all rate constants and has shown that all measurements agree with their overall linear fit within their uncertainty limits. The calculated 2σ uncertainties range in general between 20 and 50% of the rate constants, but can occasionally reach up to a factor of 2. These errors are consistent with the spread between multiple measurements at a given temperature. The obtained results clearly indicate that these two reactions have low values of k_1 and k_2 at ambient temperature associated with a positive temperature dependence in the temperature range 293−623 K. The rate constants k_1 and k_2 are independent of (i) the coating of the Knudsen cell (Halocarbon Wax or Teflon), (ii) the source of $C_2H_5^\bullet$ free radical, using either $Cl^\bullet + C_2H_6 \rightarrow C_2H_5^\bullet + HCl$ or $H^\bullet + C_2H_5I \rightarrow C_2H_5^\bullet + HI$, and (iii) the used data treatment method, based on the direct observation of either $C_2H_5^\bullet$ or the closed shell products. The linear correlation coefficients (r^2) are high for both k_1 and k_2. Therefore, all data collected under differing experimental conditions have been

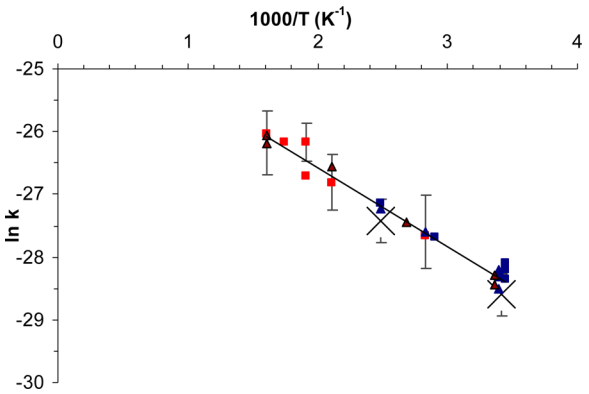

Figure 5. Arrhenius plots of k_1 ($C_2H_5^\bullet + HBr \rightarrow C_2H_6 + Br^\bullet$) for all investigated conditions presented in Table 5. Squares, C_2H_6 + Cl; triangles, C_2H_5I + H radical generation; blue symbols, Halocarbon Wax coating (15-00); red and dark red symbols, Teflon (FEP) coating; triangles with dark red background, measurements in reactor b; crosses, results obtained from closed shell product detection. Correlation parameters (solid line): $y = [-1.28(\pm0.22)]x - 24.02(\pm0.61)$, $r^2 = 0.97$.

dx.doi.org/10.1021/jp403761r | J. Phys. Chem. A XXXX, XXX, XXX−XXX

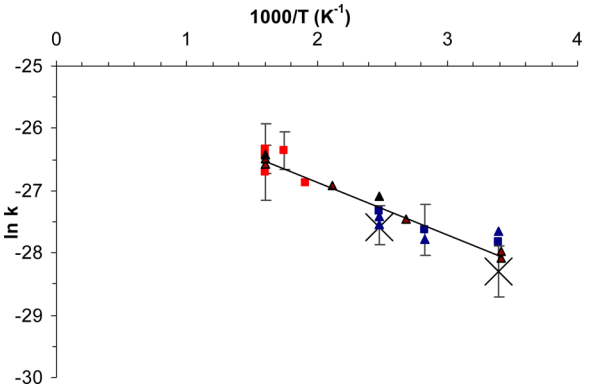

Figure 6. Arrhenius plots of k_2 ($C_2H_5^\bullet$ + HI → C_2H_6 + I$^\bullet$) for all investigated conditions presented in Table 6. Squares, C_2H_6 + Cl; triangles, C_2H_5I + H radical generation; blue symbols, Halocarbon Wax coating (15-00); red and dark red symbols, Teflon (FEP) coating; triangles with dark red background, measurements in reactor b; crosses, results obtained from closed shell product detection. Correlation parameters (solid line): $y = [-0.86(\pm0.13)]x - 25.14(\pm0.32)$, $r^2 = 0.91$.

used to determine the general Arrhenius expressions for the two investigated free radical−molecule metathesis reactions:

$$k_1 = 3.69(\pm0.95) \times 10^{-11} \exp(-10.62(\pm0.66)/RT) \quad (17)$$

$$k_2 = 1.20(\pm0.38) \times 10^{-11} \exp(-7.12(\pm1.059)/RT) \quad (18)$$

where the units are in cm^3/molecule s for pre-exponential factors and kJ/mol for the activation energies.

Uncertainties derive from a statistical treatment of the random errors of the measurement, enabling the derivation of the standard deviation associated with the slope and with the intercept of the linear regression Arrhenius plot. The indicated errors are for a statistical precision of 2σ. The possible systematic errors are judged to be small owing to the consistency of the results under all experimental conditions investigated.

As mentioned above, the good agreement between results obtained from both rate constant calculation methods supports the contention that the chemical system of interest is fully understood and all the significant reactions are taken into account in the data analysis. The good agreement between results coming from different $C_2H_5^\bullet$ generation schemes represents additional support. This leads to the conclusion that no H$^\bullet$ or Cl$^\bullet$ radicals are admitted into the Knudsen reactor from the discharge tube through the mixing region where $C_2H_5^\bullet$ radicals are produced. This was already suggested before in view of the constant MS signal of HCl and Cl_2. If this were not the case, it would mean that additional reactions having a high rate constant would compete with reactions R1 and R2. As an example, we may take a few potentially relevant and fast reactions such as the following: Cl$^\bullet$ + HI → HCl + I$^\bullet$, k(298 K) = 1.22 × 10^{-10} cm^3/molecule s;[44] H$^\bullet$ + HBr → H_2 + Br$^\bullet$, k(298 K) = 6.32 × 10^{-12} cm^3/molecule s;[45] or H$^\bullet$ + HI → H_2 + I$^\bullet$, k(298 K) = 2.09 × 10^{-13} cm^3/molecule s.[46] The competition of any of the above three reactions would be a change in the concentrations of HBr, HI, and the closed shell products, which would finally lead to a disagreement of obtained rate constants as a function of the $C_2H_5^\bullet$ generation scheme and the used data treatment method. The consistent results obtained in the present study are a strong indication that the experiments were conducted under conditions that are largely free of interfering artifacts.

Moreover, the kinetic results are not influenced by the type of lamp used as a photoionization source (Cl_2, 8.9 eV; H_2, 10.2 eV). This is an indication that no photolytic or ionization processes of importance occur in the Knudsen reactor. It is important to check the effects of the VUV light, because a thin light beam enters the reactor through its exit aperture due to the collinear geometry of the experimental device used (see Figure 1).

The fact that the wall losses are small and that the chemical system is apparently not subject to competitive secondary reactions strongly supports the underpinning of the present data, in the aftermath of improvements made on the experimental apparatus enabling the generation of thermally equilibrated radicals

Comparison with Previously Published Results. A comparison of the present Arrhenius plots with those previously published is made in Figures 7 and 8. For reaction

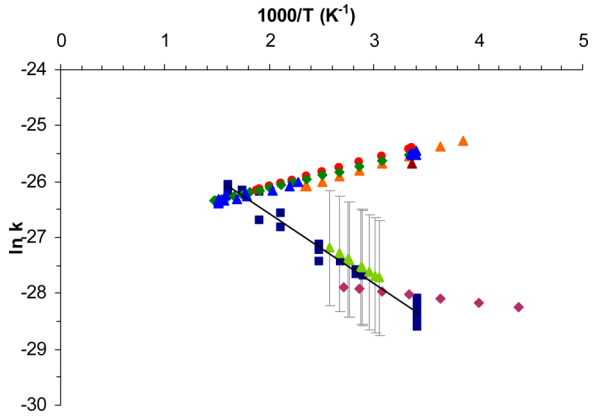

Figure 7. Comparison of the Arrhenius plot (solid line) of current data with previously published k_1 ($C_2H_5^\bullet$ + HBr → C_2H_6 + Br$^\bullet$) under the listed experimental conditions presented in Table 5. Dark blue squares, present work; orange triangles, Nicovich et al.;[12] red circles, Seakins et al.;[10] green diamonds, Seetula;[11] purple diamonds, Dobis and Benson;[14] dark blue triangles, Ferrell;[15] light green triangles, Fettis and Trotman-Dickenson[16] in combination with Hunter et al.[20] and Hayes et al.;[21] dark red triangles, Golden et al.[17] Uncertainties reflect the disagreement between the studies of Hunter et al.[20] and Hayes et al.[21]

R1, it appears that the present experiments are in close agreement with the measurement performed by Fettis and Trotman-Dickenson,[16] when new data of Hunter and Kristjansson[20] and Hayes and Strong[21] are taken into account. These authors present new data for the rate constant of the competitive reaction $C_2H_5^\bullet$ + I_2 → C_2H_5I + I$^\bullet$. Indeed, as mentioned in the Introduction, the lack of kinetic data for this last reaction at the date of publication of ref 16 has excluded an evaluation of the pre-exponential factor. Today, this difficulty may be overcome by using recently published data from Hunter and Kristjansson[20] and Hayes and Strong[21] in combination with the rate constant ratio of reaction R1 and $C_2H_5^\bullet$ + I_2.[16] In this way, a pre-exponential factor in the range 1.87 × 10^{-11}−8.45 × 10^{-11} (cm^3/molecule s) may be determined. The results obtained by Hunter and Kristjansson[20] and Hayes and Strong[21] differ by roughly an order of magnitude; therefore, the results presented in Figure 7 are an average of these two studies. The

dx.doi.org/10.1021/jp403761r | J. Phys. Chem. A XXXX, XXX, XXX−XXX

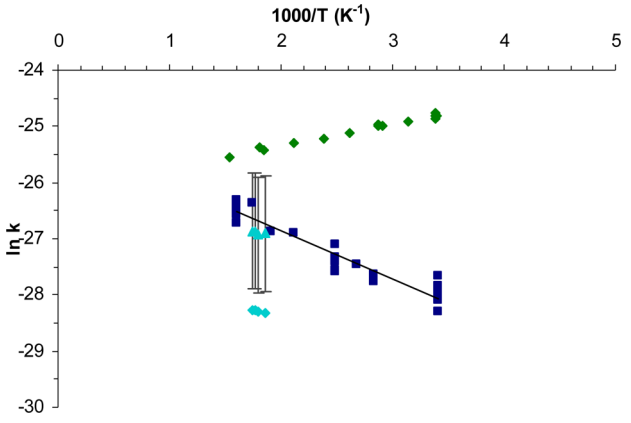

Figure 8. Comparison of the Arrhenius plot (solid line) of current data with previously published k_2 ($C_2H_5^\bullet$ + HI → C_2H_6 + $I^\bullet$) under the listed experimental conditions presented in Table 6. Dark blue squares, present work; green diamonds, Seetula et al.;[19] light blue diamonds, Hartley and Benson;[18] light blue triangles, Hartley and Benson recalculated based on work published in refs 20 and 21. Uncertainties reflect the disagreement between the studies of Hunter et al.[20] and Hayes et al.[21]

error bars are a consequence of the large uncertainties in the rate constant for the reaction of $C_2H_5^\bullet$ + I_2. The agreement with the present results is quite satisfactory, both in terms of the absolute values obtained for the rate constant and for its temperature dependence corresponding to E_a = 9.6 kJ/mol[16] compared to 10.6 kJ/mol from the present work.

Similarly, the data published by Hartley and Benson[18] concerning reaction R2 may be corrected using the more recent measurements of the rate constant for $C_2H_5^\bullet$ + I_2 → C_2H_6 + $I^\bullet$.[20,21] The recalculated rate constant k_2 leads to a significantly higher value than the one obtained by Hartley and Benson, who have extracted rate parameters from a complex chemical system using an estimated rate constant for the reaction of $C_2H_5^\bullet$ + I_2. This new evaluation is in good agreement with k_2 of the present study as displayed in Figure 8. Nevertheless, the activation energy obtained by Hartley and Benson[18] differs by a factor of 2 from results of the present work. However, the temperature range investigated in the former study[18] is too small to assess the temperature dependence of k_2 with sufficient accuracy.

The investigation of Dobis and Benson for reaction R1[14] is the only previous work performed under conditions similar to those in the present work, namely using a very low pressure reactor coupled to a "soft" chemical generation of $C_2H_5^\bullet$. The disagreement between the present results and Dobis and Benson is not very important in terms of the absolute values of the rate constant for the overlapping temperature range; however, the present results show a temperature dependence that is 5 times larger. This discrepancy may perhaps arise from a more complex chemical system in the experiments of Dobis and Benson, due to the in situ generation of the radical, in contrast to the present external free radical generation. The $Cl^\bullet$ atoms directly flow into their Knudsen reactor and may potentially undergo competing reactions other than those taken into account in their data treatment, which are $Cl^\bullet$ + HBr → HCl + $Br^\bullet$, $C_2H_5^\bullet$ + $Cl^\bullet$ → C_2H_4 + HCl, C_2H_4 + $Cl^\bullet$ → $C_2H_3^\bullet$ + HCl, and $C_2H_3^\bullet$ + $Cl^\bullet$ → C_2H_2 + HCl. In the present experiment, all $Cl^\bullet$ atoms are consumed by reaction with an excess of C_2H_6 before entering the reactor.

The major difference between the present results and those previously published, both k_1 and k_2, may be observed for all studies in which photolytic generation of the free radical using a suitable precursor such as C_2H_5I or $C_2H_5COC_2H_5$ has been used.[10−12,15,19] Indeed, much higher values of k_1 or k_2 coupled to a negative T-dependence have been measured under those conditions in contrast to the present results. At that point, a single and unambiguous explanation for this discrepancy cannot be given. In our opinion, the reason for this disagreement may most likely lie in the thermal generation of ethyl radical in the present work in contrast to photolytic production.

The use of an eximer laser to induce in situ photodecomposition of a suitable free radical precursor directly in the tubular reactor implies that the other chemical species are also irradiated by these highly energetic (up to 6.3 eV) UV photons. This may induce unexpected photodissociation which may partly be the source of artifacts such as an unwanted photoexcitation and/or photodissociation of the titrants, HBr or HI.[47,48] The photodissociation of these compounds will release $H^\bullet$ atoms that may induce competitive reactions not taken into account in the data treatment, or even lead to a fast chain reaction.

Another potential artifact of the UV photolysis may be the generation of internally excited free radicals. Indeed, all photolytic free radical generation schemes used[10−12,15,19] release large amounts of excess energy that partly remains as excitation in the photoproducts. According to energy conservation, the excess energy (E_{excess}) that the products of a photolytic process have to share may be calculated from the difference between the energy of the incident photon and the relevant bond dissociation energy of the precursor (D^0):

$$E_{excess} = h\nu - D^0 \quad (19)$$

Values for E_{excess} of the photolytic scheme used in refs 10, 11, 12, 15, and 19 are presented in Table 7, in which D^0 has been calculated from thermochemical quantities listed in the Millennium database.[28] It appears that all processes generate photofragments that have to partition energies in the range 216−280 kJ/mol into their rotational, vibrational, and translational degrees of freedom. This extra energy may enhance the chemical reactivity of the generated $C_2H_5^\bullet$ free radical with HX and may lead to subsequent chemical reaction rates that are not thermal.

In order to answer to the above criticism, the authors of these studies argued that the relaxation of free radicals occurs in

Table 7. Energies for the Photolytic Free Radical Generation

authors	λ (nm)	$h\nu$ (kJ/mol)	radical generation	D^0 [a] (kJ/mol)	E_{excess} (kJ/mol)
Nicovich et al.[12]	266	4.50×10^2	$C_2H_5I \rightarrow C_2H_5 + I$	2.34×10^2	2.16×10^2
Seakins et al.[10]	248	4.82×10^2	$CH_3COC_2H_5 \rightarrow C_2H_5 + CH_3CO$	2.49×10^2	2.34×10^2
Seakins et al.[10]	193	6.20×10^2	$C_2H_5COC_2H_5 \rightarrow C_2H_5 + C_2H_5CO$	3.40×10^2	2.80×10^2
Seetula et al.[11,19]	248	4.82×10^2	$C_2H_5I \rightarrow C_2H_5 + I$	2.34×10^2	2.49×10^2

[a]Bond scission energies have been calculated using accepted thermochemical values from Millennium database.[28]

dx.doi.org/10.1021/jp403761r | J. Phys. Chem. A XXXX, XXX, XXX−XXX

Table 8. Rate Parameters for $C_2H_6 + X^\bullet \rightarrow C_2H_5^\bullet + HX$ (X = I, Br) from the Literature

C_2H_6 + Br				
authors	T range (for k_{-1}) (K)	A_{-1} (cm^3/molecule s)	$E_{a,-1}$ (kJ/mol)	k_{-1}(450 K) (cm^3/molecule s)
Fettis et al.[50]	423−483	1.30×10^{-10}	56.0	4.10×10^{-17}
Coomber and Whittle[51]	312−394	3.25×10^{-11}	51.5	3.43×10^{-17}
King et al.[52]	494−592	6.61×10^{-10}	58.5	1.07×10^{-16}
Russell et al.[9]	298−478	7.01×10^{-10}	53.4	4.43×10^{-16}
Seakins et al.[10]	473−621	2.36×10^{-10}	53.3	1.53×10^{-16}
Ferrell[15]	448−620	3.34×10^{-10}	54.1	1.75×10^{-16}
C_2H_6 + I				
authors	T range (for k_{-2}) (K)	A_{-2} (cm^3/molecule s)	$E_{a,-2}$ (kJ/mol)	k_{-2}(550 K) (cm^3/molecule s)
Hartley and Benson[18]	536−576	2.76×10^{-10}	116.6	2.33×10^{-21}
Knox and Musgrave[53]	503−618	2.21×10^{-10}	111.0	6.34×10^{-21}

many collisions with the bath gas and sometimes with the reactor walls.[10−12,15,19] However, it should be noted that the collisional environment significantly differs in the two types of experiments. Ethyl free radicals undergo many collisions with the walls in the present system, both in the radical generation tube and in the Knudsen reactor. The many "hard" collisions with the wall in a Knudsen reactor are given by the collision frequency ω (s^{-1}) = $4386(T/M)^{1/2}$ and ω (s^{-1}) = $3509(T/M)^{1/2}$ in reactors a and b, respectively. This is in distinct contrast to the collisions that the free radicals undergo with the weak colliders He and N_2 used as bath gases.[10−12,15,19]

An additional difference between the present study and those previously published[10−12,15,19] is the magnitude of $k_w^{C_2H_5}$ for radical wall loss. The small values found in this study are in distinct contrast to those observed in the UV photolytic studies.[10−12,18] The present results lead to a measured upper limit of $k_w^{C_2H_5}$ = 1.19 s^{-1} at ambient temperature, whereas the photolytic studies often report values at least 10 times higher. These discrepancies may not be rationalized in a simple way, on the basis that identical coatings were used in some cases. Moreover, some surprising variations of $k_w^{C_2H_5}$ between two sets of experiments performed at nominally identical conditions may be noted. These observations suggest that $k_w^{C_2H_5}$ may possibly not be linked to wall loss of ethyl free radical.

The problem of high values of $k_w^{C_2H_5}$ has already been discussed in a previous paper involving the reaction of DX + *tert*-butyl free radical. The average value of $k_w^{C_2H_5}$ in the range 0.5 ± 1.5 s^{-1} obtained by Müller-Markgraf et al.[49] was also in constrast to significantly higher values obtained in studies using flash photolysis in a tubular flow reactor. Moreover, the studies of Müller-Markgraf et al.[49] provide an interesting hint to a problem that may arise from photolytic generation of the radical and the presence of excess internal energy. Indeed, the radical was generated by photolysis at both 248 and 351 nm of a suitable azo compound precursor. The results obtained at 351 nm, the lowest photon energy, has enabled the measurement of rate constants from the detection of closed shell products. However, when the incident photon energy was increased to 248 nm, the signal due to the recombination products of *tert*-butyl ceased to be observed. According to Müller-Markgraf et al.,[49] the photolysis generates vibrationally excited *tert*-butyl free radicals, whose absorption cross section at the photolysis wavelength (248 nm) is significantly enhanced with respect to its ground state, and therefore leads to fast secondary photolysis and the concomitant destruction of the *tert*-butyl free radical. In conclusion, we point out the low values of $k_w^{C_2H_5}$ obtained in this work, in agreement with previous results for the *tert*-butyl free radical obtained using a Knudsen flow reactor.[49] In addition, the temperature dependence of $k_w^{C_2H_5}$ is what is expected from basic considerations of wall desorption that is increasing with temperature.

Thermochemistry of $C_2H_5^\bullet$ Free Radical. Thermochemical calculations may be performed on the basis of the present results for the metathesis reactions of $C_2H_5^\bullet$ with HBr (k_1) or HI (k_2), and the rate constants for the reverse reactions, k_{-1} and k_{-2}, respectively. The rate constants used for the forward reaction are those obtained with the k_w corrections:

$$k_1 = 3.69(\pm 0.95) \times 10^{-11} \exp(-10.62(\pm 0.66)/RT) \quad (17)$$

$$k_2 = 1.20(\pm 0.38) \times 10^{-11} \exp(-7.12(\pm 1.059)/RT) \quad (18)$$

For reactions R1 and R2, there exist several kinetic studies on the reverse rate X (X = HBr or HI) + ethyl reactions as presented in Table 8. Therefore, calculations have been performed by using the values of k_{-1} and k_{-2} of each study, whose temperature range overlapped with k_1 and k_2, respectively, of the present study.

The standard heat of formation $\Delta_f H^\circ_{298}(C_2H_5^\bullet)$ has been calculated by both the "second" and "third law" methods using kinetic data obtained for the equilibria $C_2H_5^\bullet$ + HBr ⇆ C_2H_6 + $Br^\bullet$ and $C_2H_5^\bullet$ + HI ⇆ C_2H_6 + $I^\bullet$. The "second law" method takes the difference of the activation energies of the forward ($E_{a,i}$) and reverse ($E_{a,-i}$) reaction in order to obtain the enthalpy of reaction: ΔH°_r. This is the most direct method but is very sensitive to errors in the activation parameters. In each calculation, T_m, the temperature in the middle of the range, was used as the relevant temperature for the thermochemical calculation. The obtained $\Delta_f H^\circ_{298}$ values have subsequently been corrected in order to obtain the reaction enthalpy at 298 K using known reactant and product heat capacities and their temperature dependence[28] according to

$$\Delta_r H^\circ_{298} = E_{a,i} - E_{a,-i} - \int_{298}^{T_m} \left(\sum C_{p,\mathrm{prod}} - \sum C_{p,\mathrm{react}}\right) dT \quad (20)$$

The "second law" method enables furthermore the calculation of the reaction entropy $\Delta_r S_T$ at the mean temperature, based on the pre-exponential factors using the following equation:

$$\Delta_r S_T = R \ln\left(\frac{A_i}{A_{-i}}\right) \quad (21)$$

dx.doi.org/10.1021/jp403761r | J. Phys. Chem. A XXXX, XXX, XXX−XXX

Table 9. Thermochemical Parameters of Ethyl Free Radical from $C_2H_5^\bullet$ + HX ⇆ C_2H_6 + $X^\bullet$ Equilibria Using k_1 and k_2 from This Work and k_{-1} and k_{-2} from Works of Listed Authors[a]

		second law		third law	
authors for k_{-i}	T range (for k_{-i}) (K)	$\Delta_f H^\circ_{298}$	S°_{298}	$\Delta_f H^\circ_{298}$ (K_r at T_m)[b]	$\Delta_f H^\circ_{298}$ (K_r at 298 K)[c]
		C_2H_6 + Br			
Fettis et al.[50]	423−483	108.5[d]	216[d]	121.6[d]	117.2[d]
Coomber and Whittle[51]	312−394	104.4[d]	204[d]	118.0[d]	115.9[d]
King et al.[52]	494−592	110.7 ± 1.4	229 ± 1.3	119.4 ± 4.6	115.7 ± 2.9
Russell et al.[9]	298−478	106.1 ± 2.4	230 ± 4.6	111.6 ± 2.4	110.4 ± 1.8
Seakins et al.[10]	473−621	105.5 ± 2.3	221 ± 1.4	118.9 ± 5.7	113.0 ± 3.8
Ferrell[15]	448−620	106.2 ± 1.1	224 ± 0.5	117.3 ± 2.3	113.0 ± 1.1
average		106.9 ± 2.4	220 ± 10.1	117.8 ± 3.8	114.2 ± 2.6
		C_2H_6 + I			
Hartley and Benson[18]	536−576	105.1[d]	229[d]	114.1[d]	110.2[d]
Knox and Musgrave[53]	503−618	99.5 ± 6.4	227 ± 5.0	109.7 ± 10.4	105.2 ± 12.1
average		102.3	228	111.9	107.7
total average		105.7 ± 2.7	223 ± 7.4	116.3 ± 3.4	112.6 ± 3.1

[a]Units of $\Delta_f H^\circ_{298}$ in kJ/mol and S°_{298} in J/K mol. Thermochemical quantities for other products and reactants and S°_{298} of $C_2H_5^\bullet$ = 242.9 J/K mol for the third law calculations from Millenium database.[28] [b]Calculation based on rate constant at the mean temperature (T_m) of the inverse reaction (k_{-i}). T_m is the algebraic (unweighted) average over the temperature range. [c]Calculation based on the absolute kinetic constant at 298 K determined by extrapolation. [d]A suitable error treatment cannot be performed as the uncertainty of the inverse rate constant has not been published.

where A_i and A_{-i} are the pre-exponential factors for the forward and reverse rate constants, respectively. The absolute reaction entropy at 298 K may then be obtained using eq 22:

$$\Delta_r S_{298} = \Delta_r S_T - \int_{298}^{T_m} \frac{\sum C_{p,\mathrm{prod}} - \sum C_{p,\mathrm{react}}}{T}\,\mathrm{d}T \tag{22}$$

The "third law" calculation is based on the equilibrium constant calculated at a given temperature from the ratio of the forward (k_i) and reverse (k_{-i}) rate constants:

$$K_r = \frac{k_i}{k_{-i}} \tag{23}$$

When an accepted value for $\Delta_r S_T$ from ref 28 is inserted, the enthalpy of reaction $\Delta_r H_T$ may be calculated from eq 24:

$$\Delta_r H_T = T(\Delta S_r^\circ - R \ln K_r) \tag{24}$$

Two "third law" treatments have been performed: the first at the mean temperature T_m of k_{-I} (method a), and the second at 298 K using k_{-i} obtained by extrapolation of kinetic data measured at higher temperature (method b). In the first case, the obtained $\Delta_r H_T$ was corrected to 298 K in the same way as in the second law treatment given in eq 20.

Finally, the obtained reaction enthalpies $\Delta_r H^\circ_{298}$ and entropies $\Delta_r S_{298}$ may be used to derive the standard heat of formation of $C_2H_5^\bullet$ as thermochemical quantities when the corresponding values for the reactants and products other than $C_2H_5^\bullet$ are known:[28]

$$\Delta_f H^\circ_{298}(C_2H_5) = -\Delta_r H^\circ_{298} - \Delta_f H^\circ_{298}(HX) + \Delta_f H^\circ_{298}(X) + \Delta_f H^\circ_{298}(C_2H_6) \tag{25}$$

The results of the above calculations are all presented in Table 9, which displays the results using k_1 and k_2 of this work combined with k_{-1} and k_{-2} reported by the listed authors. The results of the "second law" treatment concerning the equilibrium $C_2H_5^\bullet$ + HBr ⇆ C_2H_6 + $Br^\bullet$ lead to an average value $\Delta_f H^\circ_{298}(C_2H_5^\bullet)$ = 106.9 ± 1.9 kJ/mol. The uncertainties reflect the slight variation in the activation energy between studies that dealt with the kinetics of k_{-1}. This average value is, within the uncertainties, in good agreement with the second law calculation for $C_2H_5^\bullet$ + HI ⇆ C_2H_6 + $I^\bullet$ using k_{-2} values published by Hartley and Benson.[18] The calculation based on results of Knox and Musgrave[53] leads to a lower value of $\Delta_f H^\circ_{298}(C_2H_5^\bullet)$ = 99.5 ± 6.4 kJ/mol owing to a low activation energy of k_{-2}. However, a 2σ Dixon's Q test indicates that this value is not an outlier from a statistical point of view and therefore has to be included in the total average of the standard enthalpy calculated according to the second law method resulting in $\Delta_f H^\circ_{298}(C_2H_5^\bullet)$ = 105.7 ± 1.9 kJ/mol. This value is significantly lower than that currently accepted and tabulated in compilations such as the Millennium database with $\Delta_f H^\circ_{298}(C_2H_5^\bullet)$ = 118.7 kJ/mol.[28] However, it agrees quite well with some older evaluations such as $\Delta_f H^\circ_{298}(C_2H_5^\bullet)$ = 108.68 kJ/mol and $\Delta_f H^\circ_{298}(C_2H_5^\bullet)$ = 105.75 ± 5.0 kJ/mol resulting from the kinetic studies of Fettis and Trotman-Dickenson[16] and Hartley and Benson,[18] respectively.

However, the "second law" absolute entropy leads to an average value S°_{298}= 223 ± 7.4 J/K mol for ethyl free radical. This value is 19.9 J/K mol lower than the currently accepted value of the Millennium database.[28] This inconsistency indicates a problem with the "second law" treatment in the present case. Therefore, we conclude that "third law" heats of formation may be more accurate in view of the fact that absolute entropies of free radicals are known from other sources.

The two "third law" assessments lead to larger values than those obtained from the "second law" treatment. The average $\Delta_f H^\circ_{298}(C_2H_5^\bullet)$ = 116.3 ± 3.4 kJ/mol obtained at T_m (method a) is slightly higher than $\Delta_f H^\circ_{298}(C_2H_5^\bullet)$ = 112.6 ± 3.1 kJ/mol obtained with method b at 298 K. In fact, the difference between the two "third law" assessments arises from the way to perform the temperature correction from the investigated experimental temperature range to 298 K. Method a uses the heat capacities of reactants and products in order to perform the temperature correction. Method b, on the other hand, requires the extrapolation of the rate constant k_{-i} from the investigated temperature range to 298 K using the published kinetic parameters A_{-i} and $E_{a,-i}$. Therefore, a suitable "third law" treatment at 298 K requires accurate knowledge of the

dx.doi.org/10.1021/jp403761r | J. Phys. Chem. A XXXX, XXX, XXX−XXX

kinetics, especially $E_{a,-i}$. The reliability of $E_{a,-i}$ depends on the size of the investigated inverse temperature range $(1/T)$ because it is obtained from simple Arrhenius plots. Table 9 reveals that, with the exception of the studies of Coomber and Whittle[51] and Russell et al.,[9] the $1/T$ range for the measurement of k_{-i} was rather narrow with a maximum and minimum variation by factors of 1.6 (1/298−1/478, Russell et al.[9]) and 1.07 (1/536−1/576, Hartley and Benson[18]) between the low and high limits.

In comparison, k_i was measured over a larger temperature range (1/298−1/623) compared to k_{-1}, corresponding to a factor of 2.1 between the two extremes including ambient temperature in this study. We conclude that E_{-i} values are more uncertain than E_i and/or the measured absolute value of k_{-1} at T_m. In order to avoid a long and quite uncertain extrapolation of k_{-1} from T_m to 298 K, we decidedly favor method a over b using well-accepted heat capacity data from the Millenium database in order to perform the temperature correction of the equilibrium constant K_r.

It may also be noted that $\Delta_f H^\circ_{298}(C_2H_5^\bullet) = 109.7 \pm 10.4$ kJ/mol obtained from the rate constant of $C_2H_6 + I^\bullet$ published by Knox and Musgrave[53] is much lower than the majority of the other results, is more uncertain (±10.4 kJ/mol), and is not within the range of $\Delta_f H^\circ_{298}(C_2H_5^\bullet) = 117.8 \pm 3.8$ kJ/mol, the average for the $C_2H_6 + Br^\bullet$ reactions. We are therefore omitting this value in our recommendation. $\Delta_f H^\circ_{298}(C_2H_5^\bullet) = 114.1$ kJ/mol obtained from the data of Hartley and Benson[18] is the only result based on the iodination system that obtains acceptable agreement with the results from the bromination system and will therefore be considered in our recommendation.

For these reasons, the recommendation we propose from the present results is $\Delta_f H^\circ_{298}(C_2H_5^\bullet) = 117.3 \pm 3.1$ kJ/mol, the average value of the third law treatments performed at T_m (method a) and omitting the results of Knox and Musgrave.[53] This value is in acceptable agreement with some previously published $\Delta_f H^\circ_{298}(C_2H_5^\bullet)$ values such as 118.6 ± 2 kJ/mol recommended by Pilling and co-workers,[6] 119.0 ± 2 kJ/mol from the compilation of Tsang,[8] or 118.7 kJ/mol from the Millennium database[28] that are based on several types of experiments using other techniques. However, it is slightly, but significantly lower than the results based on studies in which a negative activation energy has been measured.[9−12] The fact that the difference to these studies regarding the thermochemistry is not so important, albeit the kinetics of C_2H_5 + HX being completely different is not surprising. Indeed, the present recommendation is based on the ratio of the absolute rate constants k_i/k_{-i} (i.e., the equilibrium constant) at the mean temperature of the investigated range T_m which mostly corresponds to elevated temperatures where the disagreement between k_i values among all kinetic studies is minimal. In the "third law" approach the agreement between the different values of $\Delta_f H^\circ_{298}(C_2H_5^\bullet)$ is thus expected owing to the similarity of the equilibrium constant at temperatures where both types of experiments obtaining k_i, associated with positive or negative values of E_a, merge as displayed in Figures 7 and 8.

In conclusion, the results of the thermochemical analysis show that fully consistent values of $\Delta_f H^\circ_{298}(C_2H_5^\bullet)$ between second and third law evaluation, as well as between experiments using HBr and HI, may not be obtained. We emphasize, however, that, in general, the result of the present work supports a lower value of $\Delta_f H^\circ_{298}(C_2H_5^\bullet)$ compared to some of the currently accepted values. This trend toward the lower limit of the generally accepted values is consistent with the present recommendation of $\Delta_f H^\circ_{298}(C_2H_5^\bullet) = 117.3 \pm 3.1$ kJ/mol obtained using a "third law" evaluation.

CONCLUSIONS

This study provides new Arrhenius expressions of the rate constants for the metathesis reactions of the ethyl free radicals with HBr and HI. The results in the temperature range 293−623 K clearly confirm that these two reactions have low values of the second order rate constant at ambient temperature associated with a positive temperature dependence. Therefore, from a fundamental point of view, these results support that the investigated hydrogen transfer reactions are elementary in nature, and therefore occur in a single step passing through a transition state having a small barrier. However, the origin of the small positive barrier is currently not clear in view of a recent high-level theoretical calculation of k_1.[17] A new experimental methodology has been used that exhibits the following features; (i) external generation of free radicals using a chemical reaction, (ii) complete mechanism for radical reactions occurring in the Knudsen reactor, (iii) direct detection of ethyl free radical using SPIMS, and (iv) small $C_2H_5^\bullet$ free radical wall loss rate constant k_w in comparison to its escape rate constant k_e. Thermochemical analysis using the present kinetic results points toward a lower value of $\Delta_f H^\circ_{298}(C_2H_5^\bullet) = 117.3 \pm 3.1$ kJ/mol. The present work reveals elementary $H^\bullet$ atom metathesis kinetics characterized by a positive activation energy associated with a rather low rate constant for reactions of the type R + HX. The trend toward lower values of $\Delta_f H^\circ_{298}(R^\bullet)$ presented here for ethyl radical has also been observed for some other radicals that are under investigation, including *n*-propyl, isopropyl, and *tert*-butyl free radicals.

AUTHOR INFORMATION

Notes

The authors declare no competing financial interest.

ACKNOWLEDGMENTS

Generous support by the Swiss State Secretariat for Education, Research and Innovation (SERI) through Contract No. SBF Nr. C11.0052 in the framework of COST Project CM0901 (Detailed Chemical Kinetic Models for Cleaner Combustion) is gratefully acknowledged. We have enjoyed substantial discussions and exchanges with John Barker and David Golden over the years, both of whom sustained our enthusiasm and pushed for an in-depth reinvestigation of an "old" problem in chemical kinetics.

REFERENCES

(1) Kohse-Höinghaus, K.; Oßwald, P.; Cool, T. A.; Kasper, T.; Hansen, N.; Qi, F.; Westbrook, C. K.; Phillip, R.; Westmoreland, P. E. Biofuel Combustion Chemistry: From Ethanol to Biodiesel. *Angew. Chem., Int. Ed.* **2010**, *49*, 3572−3597.

(2) Berkowitz, J.; Ellison, G. B.; Gutman, D. Three Methods To Measure RH Bond Energies. *J. Phys. Chem.* **1994**, *98*, 2744−2765.

(3) McMillen, D. F.; Golden, D. M. Hydrocarbon Bond Dissociation Energies. *Annu. Rev. Phys. Chem.* **1982**, *33*, 493−532.

(4) O'Neal, H. E.; Benson, S. W. *Thermochemistry of Free Radicals in Free Radicals*, Kochi, J. K., Ed.; John Wiley and Sons, Inc.: New York, 1973; Vol. II, Chapter 17.

(5) Szwarc, M. The Determination of Bond Dissociation Energies by Pyrolytic Methods. *Chem. Rev.* **1950**, *47*, 75−173.

(6) Brouard, M.; Lightfoot, P. D.; Pilling, M. J. Observation of Equilibration in the System $H^{\bullet} + C_2H_4 \leftrightarrows C_2H_5^{\bullet}$. The Determination of the Heat of Formation of $C_2H_5^{\bullet}$. *J. Phys. Chem.* **1986**, *90*, 445−450.
(7) Tsang, W. Thermal Stability of Hydrocarbon Radicals. *Prepr. Symp.—Am. Chem. Soc., Div. Fuel Chem.* **1999**, *44* (3), 423−427, http://www.anl.gov/PCS/acsfuel/preprint%20archive/Files/Vol.s/Vol44-3.pdf.
(8) Tsang, W. Heats of Formation of Organic Free Radicals by Kinetic Methods. In *Energetics of Organic Free Radicals*; Simões, J. A. M., Greenberg, A., Liebman, J. F., Eds.; Structure, Energetics and Reactivity in Chemistry Series (SEARCH) 5; Blackie Academic and Professional: London, 1996.
(9) Russell, J. J.; Seetula, J. A.; Gutman, D. Kinetics and Thermochemistry of CH_3, C_2H_5, and i-C_3H_7. Study of the Equilibrium R + HBr ⇆ R-H + Br. *J. Am. Chem. Soc.* **1988**, *110*, 3092−3099.
(10) Seakins, P. W.; Pilling, M. J.; Niiranen, J. T.; Gutman, D.; Krasnoperov, L. N. Kinetics and Thermochemistry of R + HBr ⇆ R-H + Br Reactions: Determinations of the Heat of Formation of C_2H_5, i-C_3H_7, sec-C_4H_9 and t-C_4H_9. *J. Phys. Chem.* **1992**, *96*, 9847−9855.
(11) Seetula, J. Kinetics and Thermochemistry of the R + HBr ⇆ RH + Br (R = C_2H_5 or β-C_2H_4Cl) Equilibrium. An *Ab Initio* Study of the Bond Energies in Partly Chlorinated Ethanes and Propanes. *J. Chem. Soc., Faraday Trans.* **1998**, *94*, 891−898.
(12) Nicovich, J. M.; van Dijk, C. A.; Kreutter, K. D.; Wine, P. H. Kinetics of the Reactions of Alkyl Radicals with HBr. *J. Phys. Chem.* **1991**, *95*, 9890−9896.
(13) Benson, S. W.; Dobis, O. Existence of Negative Activation Energies in Simple Bimolecular Metathesis Reactions and Some Observation on Too-Fast Reactions. *J. Phys. Chem. A* **1998**, *102*, 5175−5181.
(14) Dobis, O.; Benson, S. W. Temperature Coefficients of Rates of Ethyl Radical Reactions with HBr and Br in the 228−368 K Temperature Range. *J. Phys. Chem. A* **1997**, *101*, 6030−6042.
(15) Ferrell, V. M. *Experimental Studies of the Kinetics and Thermochemisty of the Reaction Br + C_2H_4 ⇆ C_2H_4Br and Br + C_2H_6 ⇆ C_2H_5 + HBr*. Master's Thesis, Department of Chemistry, Georgia Institue of Technology, Atlanta, 1998
(16) Fettis, G. C.; Trotman-Dickenson, A. F. The Reaction of Methyl and Ethyl Radicals with Hydrogen Bromide and the Strength of C-H Bonds. *J. Chem. Soc.* **1961**, 3037−3041.
(17) Golden, D. M.; Peng, J.; Goumri, A.; Yuan, J.; Marshall, P. Rate Constant for the Reaction C_2H_5 + HBr → C_2H_6 + Br. *J. Phys. Chem. A* **2012**, *116*, 5847−5855.
(18) Hartley, D. B.; Benson, S. W. Kinetics of the Reaction of HI with Ethyl Iodide and the Heat of Formation of the Ethyl Radical. *J. Chem. Phys.* **1963**, *39*, 132−137.
(19) Seetula, J. A.; Russell, J. J.; Gutman, D. Kinetics and Thermochemistry of the Reactions of Alkyl Radicals (CH_3, C_2H_5, i-C_3H_7, s-C_4H_9 and t-C_4H_9) with HI: A Reconciliation of the Alkyl Radical Heat of Formation. *J. Am. Chem. Soc.* **1990**, *112*, 1347−1353.
(20) Hunter, T. F.; Kristjansson, K. S. Optoacoustic Method of Measuring Reaction Rates of the Radicals CH_3, CD_3, C_2H_5 and CH_2I with I and I_2. *J. Chem. Soc., Faraday Trans.* **1982**, *78*, 2067−2076.
(21) Hayes, D. M.; Strong, R. L. Secondary reactions following flash photodissociation of iodoethane and 1-iodopropane. *J. Phys. Chem.* **1986**, *90*, 6305−6309.
(22) Sato, H. Photodissociation of Simple Molecules in the Gas Phase. *Chem. Rev.* **2001**, *101*, 2687−2726.
(23) Dobis, O.; Benson, S. W. Reaction of C_2H_5 Radicals with HBr and Br at 298 K and Millitorr Pressures. *J. Am. Chem. Soc.* **1995**, *117*, 8171−8179.
(24) Benson, S. W.; O'Neal, E. Kinetics of the Reactions of Alkyl Iodides with HI. *J. Chem. Phys.* **1961**, *34* (2), 514−520.
(25) Sullivan, J. H. The Thermal Reactions of Hydrogen Iodide with Alkyl Iodide. *J. Phys. Chem.* **1961**, *65*, 722−727.
(26) Chen, Y.; Tschuikow-Roux, E. Mechanism of Hydrogen Abstraction Reaction by Free Radicals: Simple Methatesis or Involving Intermediate Complex? *J. Phys. Chem.* **1993**, *97*, 3742−3749.
(27) Sheng, L.; Li, Z.-S.; Liu, J.-Y.; Xiao, J.-F.; Sun, C. C. Theoretical Study on the Rate Constants for the C_2H_5 + HBr → C_2H_6 + Br Reaction. *J. Comput. Chem.* **2004**, *25*, 423−428.
(28) Burcat, A.; Ruscic, B. *Third Millenium ideal Gas and Condensed Phase Thermochemical Database for Combustion with Updates from Active Thermochemical Tables, Argonne National Laboratory*; Report ANL-05/20 and Technion Report TAE 960, 2005. See also: http://garfield.chem.elte.hu/Burcat/burcat.html.
(29) Timonen, R. S.; Gutman, D. Kinetics of the Reactions of Methyl, Ethyl, Isopropyl, and tert-Butyl Radicals with Molecular Chlorine. *J. Phys. Chem.* **1986**, *90*, 2987−2991.
(30) Timonen, R. S.; Russell, J. J.; Sarzynski, D.; Gutman, D. Kinetics of the Reaction of Unsaturated Hydrocarbon Free Radicals (Vinyl, Allyl, and Propargyl) with Molecular Chlorine. *J. Phys. Chem.* **1987**, *91*, 1873−1877.
(31) Castelhano, A. L.; Griller, D. Heats of Formation of Some Simple Alkyl Radicals. *J. Am. Chem. Soc.* **1982**, *104*, 3655−3659.
(32) Pacey, P. D.; Wimalasena, J. H. Kinetics and Thermochemistry of the Ethyl Radical. The Induction Period in the Pyrolysis of Ethane. *J. Phys. Chem.* **1984**, *88*, 5657−5660.
(33) Cao, J.-R.; Back, M. H. The heat of formation of the ethyl radical. *Int. J. Chem. Kinet.* **1984**, *16*, 961−966.
(34) Parmar, S. S.; Benson, S. W. Kinetics and Thermochemistry of the Reaction $Cl^{\bullet} + C_2D_6 \leftrightarrows C_2D_5^{\bullet}$ + DCl. The Heat of Formation of the $C_2D_5^{\bullet}$ and $C_2H_5^{\bullet}$ Radicals. *J. Am. Chem. Soc.* **1989**, *111*, 57−61.
(35) Ruscic, B.; Berkowitz, J.; Curtiss, L. A.; Pople, J. A. The ethyl radical: Photoionization and theoretical studies. *J. Chem. Phys.* **1989**, *91*, 114−121.
(36) Hanning-Lee, M. A.; Green, N. J. B.; Pilling, M. J.; Robertson, S. H. Direct Observation of Equilibration in the System H + C_2H_4 ⇆ $C_2H_5^{\bullet}$: Standard Enthalpy of Formation of the Ethyl Radical. *J. Phys. Chem.* **1993**, *97*, 860−870.
(37) Bödi, A.; Kercher, J. P.; Bond, C.; Meteesatien, P.; Sztaray, B.; Baer, T. Photoion Photoelectron Coincidence Spectroscopy of Primary Amine RCH_2NH_2 (R = H, CH_3, C_2H_5, C_3H_7, i-C_3H_7): Alkylamine and Alkyl Radical Heats of Formation by Isodesmic Reaction Networks. *J. Phys. Chem. A* **2006**, *110*, 13425−13433.
(38) Golden, D. M.; Spokes, G. N.; Benson, S. W. Very Low-Pressure Pyrolysis (VLPP); A Versatile Kinetic Tool. *Angew. Chem., Int. Ed.* **1973**, *12*, 534−546.
(39) Data from NIST Standard Reference Database 69: NIST Chemistry WebBook. http://webbook.nist.gov/chemistry/.
(40) Leplat, N.; Rossi, M. J. *Rev. Sci. Instrum.* **2013**, accepted.
(41) Dillon, R. T.; Young, W. G. The Preparation of Anhydrous Hydrogen Iodide. *J. Am. Chem. Soc.* **1929**, *51*, 2389−2391.
(42) Manion, J. A.; Huie, R. E.; Levin, R. D.; Burgess, D. R., Jr.; Orkin, V. L.; Tsang, W.; McGivern, W. S.; Hudgens, J. W.; Knyazev, V. D.; Atkinson, D. B.; et al. NIST Chemical Kinetics Database, NIST Standard Reference Database 17, Version 7.0 (Web version); Release 1.4.3, data version 2008.12. National Institute of Standards and Technology: Gaithersburg, MD. http://kinetics.nist.gov/.
(43) Dobis, O.; Benson, S. W. Temperature Coefficients of the Rates of Cl Atom Reactions with C_2H_6, C_2H_5 and C_2H_4. The Rates of Disproportionation and Recombination of Ethyl Radicals. *J. Am. Chem. Soc.* **1991**, *113*, 6377−6386.
(44) Yuan, J.; Misra, A.; Goumri, A.; Shao, D. D.; Marshall, P. Kinetic Studies of the Cl Plus HI Reaction Using Three Techniques. *J. Phys. Chem. A* **2004**, *108*, 6857−6862.
(45) Seakins, P. W.; Pilling, M. J. Time-Resolved Study of H + HBr → Br + H_2 and Reanalysis of Rate Data for the H_2 + Br_2 Reaction over the Temperature Range 214−1700 K. *J. Phys. Chem.* **1991**, *95*, 9878−9881.
(46) Vasileiadis, S.; Benson, S. W. Kinetics of the Reaction: H + HI → H_2 + I at 298 K and Very Low Pressures. *Int. J. Chem. Kinet.* **1997**, *29*, 915−925.
(47) Pouilly, B.; Monnerville, M. New Investigation of the Photodissociation of the HBr Molecule: Total Cross-Section, Anisotropy Parameter and Dependence of the Spin-Orbit Branching

on the Ground State Vibrational Level. *Chem. Phys.* **1998**, *238*, 437−444.
(48) Alekseyev, A. B.; Liebermann, H.-P.; Kokh, D. B.; Buenker, R. J. On the Ultraviolet Photofragmentation of Hydrogen Iodide. *J. Chem. Phys.* **2000**, *113*, 6174−6185.
(49) Müller-Markgraf, W.; Rossi, M. J.; Golden, D. M. Rate Constants for the Reaction t-C_4H_9 + DX → i-C_4H_9D + X (X = Br, I), 295 < T (K) < 384: Heat of formation of the tert-Butyl Radical. *J. Am. Chem. Soc.* **1989**, *111*, 956−962.
(50) Fettis, G. C.; Knox, J. H.; Trotman-Dickenson, A. F. The Reaction of Bromine Atoms with Alkanes and Methyl Halides. *J. Chem. Soc. A* **1960**, 4177−4185.
(51) Coomber, J. W.; Whittle, E. Bromination of Fluoro-Alkanes. *Trans. Faraday Soc.* **1966**, *62*, 1553−1559.
(52) King, K. D.; Golden, D. M.; Benson, S. W. Absolute Rate Constants and Arrhenius Parameters for the Reaction of Bromine Atoms with Ethane. *Trans. Faraday Soc.* **1970**, *66*, 2794−2799.
(53) Knox, J. H.; Musgrave, R. H. Iodination of Alkanes: Ethane, Propane and Isobutane. *Trans. Faraday Soc.* **1967**, *63*, 2201−2216.